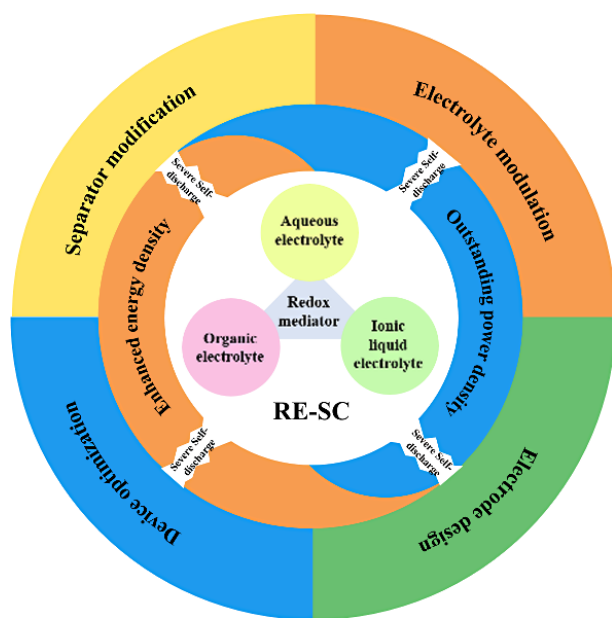



## Review

# Redox electrolyte-enhanced carbon-based supercapacitors: recent advances and future perspectives

Jiyong Shi, Xiaodong Tian , Yan Song , Tao Yang, Shengliang Hu , and Zhanjun Liu

## Graphical Abstract



 Address correspondence to Xiaodong Tian, [tianxiaodong0124@163.com](mailto:tianxiaodong0124@163.com); Yan Song, [yansong1026@126.com](mailto:yansong1026@126.com); Shengliang Hu, [hsliang@yeah.net](mailto:hsliang@yeah.net)

**Received:** September 20, 2023

**Revised:** October 15, 2023

**Accepted:** October 16, 2023

<https://www.sciopen.com/journal/3005-3315>

<https://mc03.manuscriptcentral.com/emd>

The construction of redox electrolyte-enhanced supercapacitors (RE-SCs) is an effective way to achieve high energy density without sacrificing the power output. However, this kind of device usually brings more severe self-discharge than the conventional ones. This review comprehensively summarizes the recent progress in RE-SCs. We highlighted the impacts of redox-electrolyte on the self-discharge behavior and mechanism. The suppression strategies are analyzed in terms of separator, electrolyte, electrode modification and the device optimization.

**Citation:** Shi J., Tian X., Song Y., et al. Redox electrolyte-enhanced carbon-based supercapacitors: recent advances and future perspectives. *Energy Mater. Devices*, 2023, 1, 9370009. <https://doi.org/10.26599/EMD.2023.9370009>

# Redox electrolyte-enhanced carbon-based supercapacitors: recent advances and future perspectives

Jiyong Shi<sup>1,2</sup>, Xiaodong Tian<sup>1,3</sup> ✉, Yan Song<sup>1,3</sup> ✉, Tao Yang<sup>1</sup>, Shengliang Hu<sup>2</sup> ✉, and Zhanjun Liu<sup>1,3</sup>

<sup>1</sup> CAS Key Laboratory for Carbon Materials, Institute of Coal Chemistry, Chinese Academy of Sciences, Taiyuan 030001, China

<sup>2</sup> North University of China, Taiyuan 030051, China

<sup>3</sup> Center of Materials Science and Optoelectronics Engineering, University of Chinese Academy of Sciences, Beijing 100049, China

Received: September 20, 2023 / Revised: October 15, 2023 / Accepted: October 16, 2023

## ABSTRACT

With the continuous advancement in the dual-carbon strategy, the upswell in the demand for renewable energy sources has motivated extensive research on the development of novel energy storage technologies. As a new type of energy storage device, carbon-based redox-enhanced supercapacitors (RE-SCs) are designed by employing soluble redox electrolytes into the existing devices, exploiting the merits of the diffusion-controlled faradaic process of the redox electrolyte at the surface of carbon electrodes, thus leading to improved energy density without the cost of power density. During the past years, great progress has been made in the design of novel redox electrolytes and the configuration of new devices. However, the development of these systems is plagued by severe self-discharge. Herein, a comprehensive picture of the fundamentals, together with a discussion and outline of the challenges and future perspectives of RE-SCs, are provided. We highlight the impacts of redox electrolytes on capacitance, energy density, and power output. Notably, the self-discharge behavior owing to the introduction of redox electrolyte and its mechanism are also discussed, followed by a summary of the strategies from materials to system optimization. Furthermore, possible directions for future research are discussed.

## KEYWORDS

supercapacitor, carbon materials, self-discharge, redox electrolyte

## 1 Introduction

With the rapid advancement of carbon neutrality and carbon peaking strategy, the storage of large-scale clean energy and renewal of consumer electronics have introduced higher requirements for new energy storage devices. Both secondary batteries and carbon-based supercapacitors (SCs) are the main energy storage devices currently in operation<sup>[1, 2]</sup>. Generally, batteries exhibit high energy density; however, the energy fails to convert into sufficient utilization power due to slow ion kinetics, indicating massive energy support is further needed in a very short period<sup>[3]</sup>. By contrast, SCs with outstanding power density and ultra-long life expectancy suffer from

inferior energy density due to the electrostatic adsorption mechanism at the electrode/electrolyte interface<sup>[4]</sup>. Although the energy density of SCs can be effectively increased by using pseudocapacitive materials<sup>[5-7]</sup> via surface-controlled faradaic reactions, it happens at the cost of power output and lifespan of the device because of the intrinsic features of poor electrical conductivity and low structural stability<sup>[8, 9]</sup>. Therefore, given the increasing demand for a novel electrochemical energy storage system with high energy density as well as rapid ion kinetics, it is urgently required to design a novel device in an expedient manner.

Fortunately, this dilemma can be addressed by transferring the substances undergoing redox reac-

✉ Address correspondence to Xiaodong Tian, [tianxiaodong0124@163.com](mailto:tianxiaodong0124@163.com); Yan Song, [yansong1026@126.com](mailto:yansong1026@126.com); Shengliang Hu, [hsliang@yeah.net](mailto:hsliang@yeah.net)

© The Author(s) 2023. Published by Tsinghua University Press. The articles published in this open access journal are distributed under the terms of the Creative Commons Attribution 4.0 International License (<http://creativecommons.org/licenses/by/4.0/>), which permits use, distribution and reproduction in any medium, provided the original work is properly cited.

tions from solid to liquid electrolyte<sup>[10]</sup>. Reportedly, the ion diffusion rate of redox-active species is about seven orders of magnitude higher in liquids than in solids<sup>[11]</sup>. Therefore, the construction of a redox electrolyte-enhanced SC (RE-SC) device by introducing soluble redox-active additive into the insert supporting electrolyte is considered a promising approach to achieve high energy and power densities simultaneously<sup>[12]</sup>. RE-SC has amassed broad interests due to the following advantages: (i) redox electrolyte preparation is simple and easy to scale up and conventional SC assembly process can be directly used to prepare an RE-SC device; (ii) easy-to-fabricate carbon-based electrodes can be adopted instead of complex synthesized solid-state pseudocapacitive materials; (iii) redox reaction occurs at the electrode–electrolyte interface, which is conducive to high power performance and long cycling life; and (iv) the electrochemical performance can be easily manipulated by adjusting the concentration and/or optimizing the chemical structure of redox mediators<sup>[13]</sup>.

Normally, RE-SC stores energy through both electric double-layer capacitance and faradaic capacitance streaming from soluble redox couples at the electrode–electrolyte interface on high-surface-area electrodes. As shown in Fig. 1, ether-oxidized redox-active species ( $O_{\text{bulk}}$ ) or reduced redox-active species ( $R_{\text{bulk}}$ ) in the bulk solution are first entrapped into the pores of the carbon electrodes to form  $O_{\text{pore}}$  and  $R_{\text{pore}}$  via processes 1 and 1', respectively. Subsequently, they are transformed into the transition states ( $O^*$  and  $R^*$ ) via processes 2 and 2', respectively, prior to the electron transfer. Subsequently, the  $O^*$  and  $R^*$  species are converted into their adsorbed states ( $O_{\text{ads}}$  and  $R_{\text{ads}}$ ), which further combine with electrons through process 4, leading to enhanced charge storage capacity. Notably, the  $O_{\text{ads}}$  and  $R_{\text{ads}}$  are prone to conversion into soluble states and diffusion into the bulk solution, causing the baffling concern of self-discharge<sup>[14]</sup>.

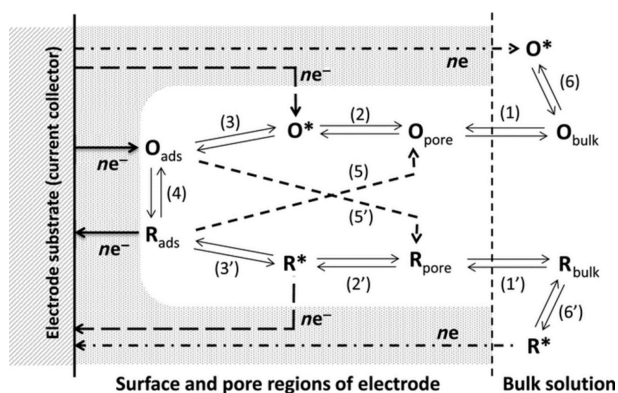


**Figure 1** Illustration of the charge storage mechanism of porous carbon-based redox-enhanced supercapacitors (RE-SC)<sup>[14]</sup>. Copyright 2015, IOP Publishing.

To date, the research studies on carbon-based RE-SCs have mushroomed rapidly and gratifying results have been achieved<sup>[15–19]</sup>. However, every coin has two sides. The fast charge capability offers outstanding advantages and causes a fatal problem, namely self-discharge, which remains as a tough nut limiting the commercial application of carbon-based RE-SCs. In a sense, self-discharge is a bigger concern than energy density because it makes RE-SCs unsuitable for applications where continuous power supply is not required. Unfortunately, little attention has been paid to the methods for inhibiting the self-discharge of RE-SC systems<sup>[20]</sup>.

In this review, recent progress on carbon-based RE-SCs is summarized with an emphasis on the development of redox-active species application in different supporting electrolytes (i.e., aqueous, organic, and ionic liquid electrolytes). Subsequently, special attention is paid to the causes of self-discharge and the corresponding suppression strategies from the separator modification, electrolyte modulation, electrode design, and device optimization comprehensively (Fig. 2). Finally, the remaining challenges and future perspectives are identified. This work can motivate further fundamental research on the development of RE-SCs and push them toward commercialization.

## 2 Development of RE-SCs

In 2005, Tanahashi reported the enhancement of the SC capacitance by adding  $\text{AgNO}_3$  into an aqueous  $\text{H}_2\text{SO}_4$  electrolyte; it marked the birth of the first RE-SC<sup>[21]</sup>. Although the development of RE-SC is still in its infancy, various species with redox activities ranging from inorganic soluble salt to organic small molecular species were tested to improve the overall performance of carbon-based SCs<sup>[22–25]</sup>. As illustrated in Fig. 3a, we summarize the major development of some redox mediators in chronological order, featuring varied ionic conductivity, redox activity, redox potential, and reversibility. Notably, the number of published papers related to carbon-based RE-SCs has rapidly increased in the past decade (Fig. 3b). Through these meaningful studies, one can infer that the optimal match between redox-active species and supporting electrolyte is of vital importance for the overall performance of an RE-SC device. The pore size distribution (PSD) and surface functionalization of the carbon electrode also affect the efficacy of redox-active species through confinement effect and bonding. In this section, the electrochemical performance of the RE-involved SCs is discussed, and the synergistic effect of the coupling of RE-porous carbon electrodes is also emphasized.

### 2.1 Aqueous redox electrolyte

Aqueous electrolytes have the advantages of high

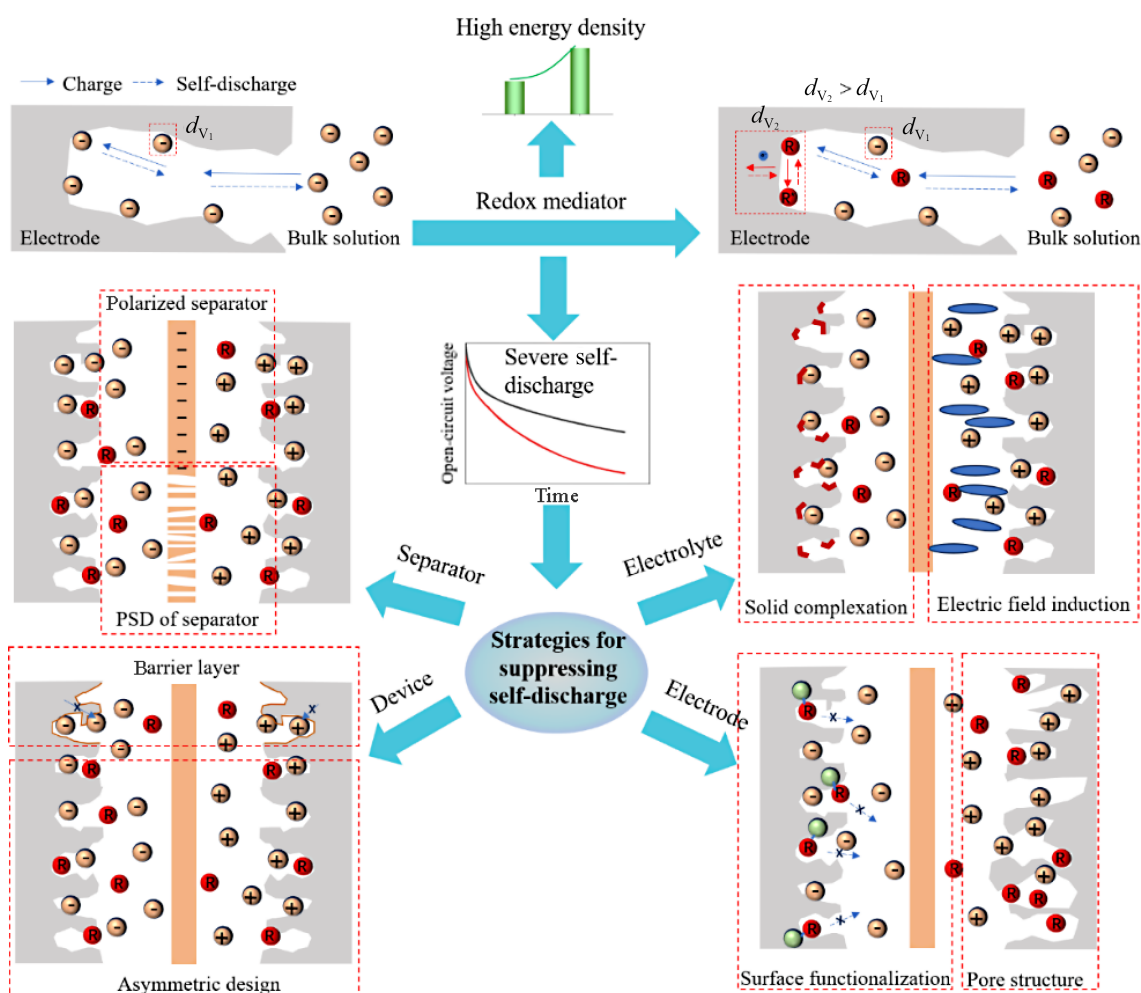


**Figure 2** Illustration of the mechanism of severe self-discharge in redox electrolyte and the strategies for suppressing it.

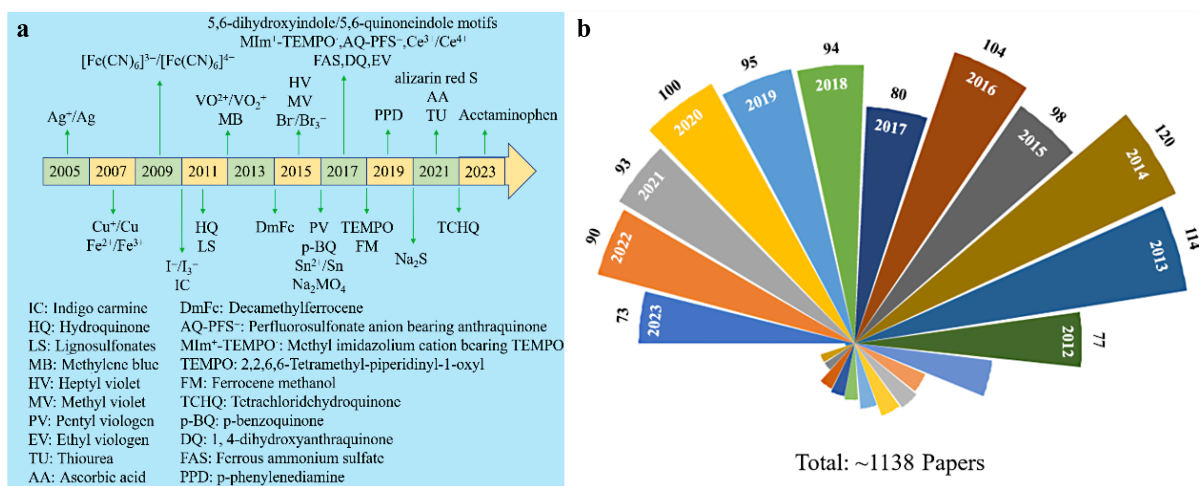


**Figure 3** (a) Timeline for the development of carbon-based redox-enhanced supercapacitors (RE-SCs); (b) Number of published papers regarding carbon-based RE-SCs in the past decade. The data were collected from Web of Science with keywords “Redox electrolyte” and “carbon-based supercapacitors”.

ionic conductivity, low viscosity, incombustibility, and low cost, which ensure high power density at low cost for the assembled device<sup>[26]</sup>. Various inorganic/organic redox-active additives were directly dissolved into aqueous supporting elec-

trolytes to augment the RE-SCs’ performance via different redox reactions<sup>[10, 16, 17, 27]</sup>.

### 2.1.1 Inorganic redox mediator

To date, numerous soluble salts, such as KI<sup>[28]</sup>, KBr<sup>[29]</sup>,

$K_3Fe(CN)_6$ <sup>[30]</sup>,  $Na_2MoO_4$ <sup>[31]</sup>, ferrous ammonium sulfate<sup>[22]</sup>, and  $NH_4VO_3$ <sup>[32]</sup>, have been dissolved in aqueous electrolytes to augment the capacity of as-fabricated devices. For example, Chen et al. introduced  $K_3Fe(CN)_6$  to  $Na_2SO_4$  electrolyte and achieved a five times increase in specific capacitance due to the additional Faraday reaction of the  $[Fe(CN)_6]^{3-}/[Fe(CN)_6]^{4-}$  redox couple<sup>[33]</sup>. Wang and coworkers further verified that the redox reaction of  $[Fe(CN)_6]^{3-}/[Fe(CN)_6]^{4-}$  could be enhanced by the catalytic reaction of hydroxyl and carbonyl functional groups on carbon surface (Fig. 4a)<sup>[30]</sup>. A strong covalent bond formed within S-containing groups, and the  $Na_2S$  additive could act as a “bridge” to accelerate the  $Na_2S$ -involved faradaic reactions (Fig. 4b). Owing to the synergistic action of S-containing groups on the carbon surface and  $S^{2-}$  in the  $Na_2S$  mediator, a high capacitance of  $643\text{ F g}^{-1}$  was obtained even at a high current load of  $15\text{ A g}^{-1}$ . Furthermore, a high energy density of  $12.6\text{ Wh kg}^{-1}$ , about 1.8 times that of the cell containing pure KOH supporting electrolyte was also achieved<sup>[34]</sup>.

Similar to using redox-active species with multiple redox centers, mixing different RE additives could also improve the capacity through the synergistic

effect of these redox-active species. Considering the mixture of  $Na_2MoO_4$  and KI as an example, as shown in Fig. 4c, the CV integral area is substantially larger than that of individual systems due to the formation of  $(Mo_xI_yO_{4x})^n-C_z$ . After adding the same dosages of  $Na_2Mo_4$  and KI into  $H_2SO_4$  supporting electrolyte, a 17.4-time enhancement in capacitance was achieved<sup>[31]</sup>.

Interestingly, both mass spectroscopy and Raman spectrometry confirmed the formation of  $IO_3^-$  ion from  $I^-$  after charging in KI + KOH electrolyte; the coexistence of  $IO_3^-/I^-$  catholyte couple and  $H_2O/H_{ad}$  redox pair allows the RE-SC to operate safely at 1.6 V with specific energy and power density comparable to those of the state-of-the-art nonaqueous electrochemical capacitors<sup>[35]</sup>.

### 2.1.2 Organic redox mediator

Organic redox mediators have gained particular attention due to their designable molecule structure, which may result in the modulation of redox potential, solubility, and electrochemical reactivity<sup>[10]</sup>. Nowadays, many soluble organic redox-active additives, such as hydroquinone (HQ)<sup>[36]</sup>, 1, 4-dihydroxyanthraquinone (DQ)<sup>[37]</sup>, pentyl viologen (PV)<sup>[38]</sup>,

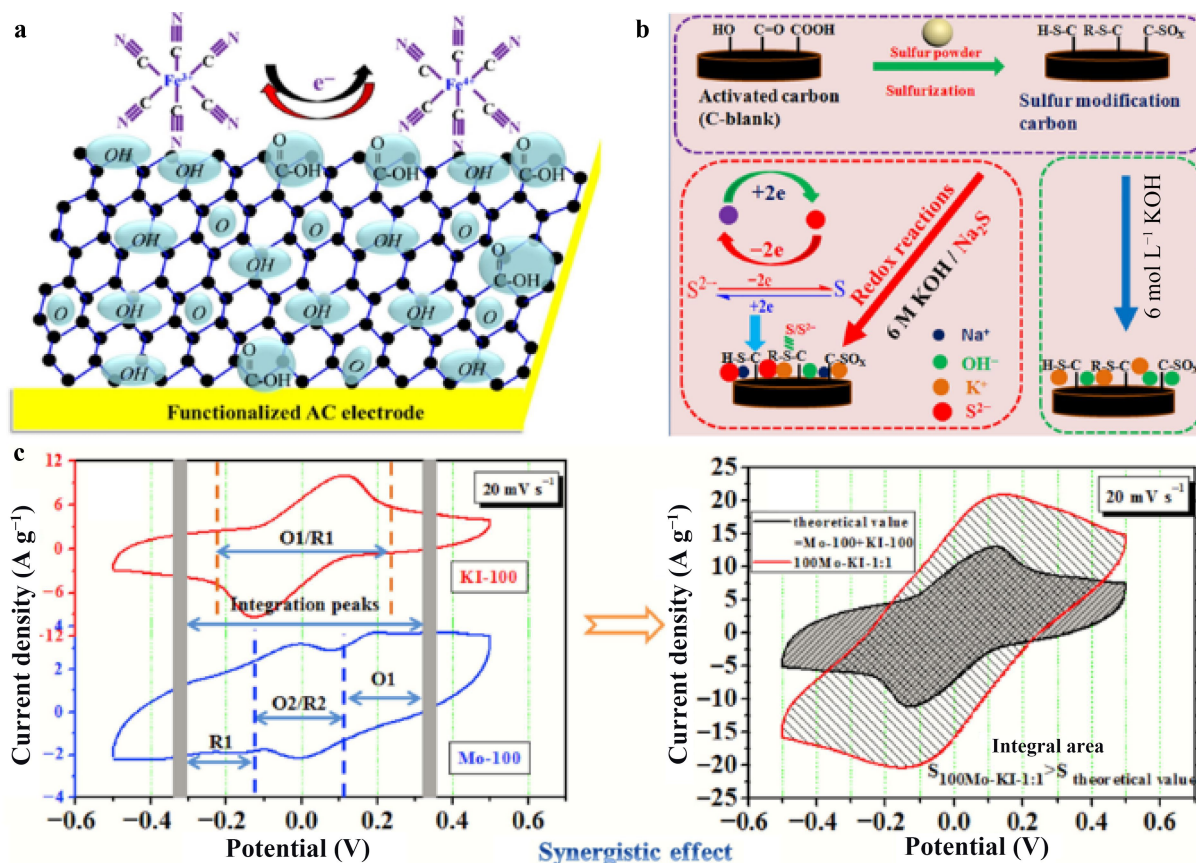


**Figure 4** (a) Illustration of the synergistic interaction between surface-oxygen functional groups and  $[Fe(CN)_6]^{3-}/[Fe(CN)_6]^{4-}$ <sup>[30]</sup>. Copyright 2018, Elsevier. (b) Diagrammatic sketch of the modification of porous carbon with the incorporation of redox additives<sup>[34]</sup>. Copyright 2020, Elsevier. (c) The synergistic effect of KI and  $Na_2MoO_4$  using the CV curves at a scan rate of  $20\text{ mV s}^{-1}$ : (left) Mo-100 and KI-100 samples; (right) theoretical value and 100Mo-KI-1:1 samples<sup>[31]</sup>. Copyright 2017, Elsevier.

2,2,6,6-tetramethylpiperidinyloxy (TEMPO)<sup>[39]</sup>, alizarin red S<sup>[40]</sup>, p-phenylenediamine (PPD)<sup>[41]</sup>, and thiourea (TU)<sup>[42]</sup>, are being frequently reported.

Yoon investigated the influence of HQ concentration on the capacitance of the as-prepared device. They found that a maximum capacitance value of 513 F g<sup>-1</sup> could be realized when 0.38 mol L<sup>-1</sup> HQ was adopted<sup>[43]</sup>. Subsequently, Chen's group evidenced the feasibility of using HQ and DQ together, and the results showed that the cooperative effect resulting from the redox processes of DQ and HQ consecutively occurring in the carbon electrode and aqueous H<sub>2</sub>SO<sub>4</sub>-supporting electrolyte could largely elevate the capacitive performance of RE-SCs<sup>[37]</sup>. An extensively conjugated indole-based macromolecule comprising 5,6-dihydroxyindole/5,6-quinoneindole motifs was prepared and used as a redox additive<sup>[44]</sup>. The narrow HOMO-LUMO gap of 2.08 eV endows SC with excellent electronic transfer kinetics. The assembled RE-SC delivers a high power density of 153 kW kg<sup>-1</sup> with a respectable energy density of 8.8 Wh kg<sup>-1</sup> along with an outstanding cycling stability (97.1% capacitance retention after 20,000 cycles). However, the conjugation degree of the redox mediator must be carefully considered to balance the stability and power output.

Despite the great process, it is difficult to find a redox mediator that can increase the capacitance for two electrodes simultaneously. Hu et al. first introduced ambipolar TEMPO into electrolyte. The results demonstrated that TEMPO contributed extra pseudocapacitance via oxidation at the positive electrode and reduction at the negative electrode simultaneously. The device with TEMPO additive delivers a high energy density of 51 Wh kg<sup>-1</sup>, 2.4 times of that without TEMPO<sup>[39]</sup>. This work highlights a new path to augment the energy density of SCs by exploring dual-functional redox-active additives.

## 2.2 Organic redox electrolyte

Considering the wide operating voltage, organic electrolyte is typically utilized in commercial SCs; thus, it is imperative to develop the redox additives suitable for organic electrolyte system to further improve the energy density of such devices.

Kim et al. added redox-active decamethylferrocene (DmFc) in an organic electrolyte, through which the energy density could be significantly increased up to 36.8 Wh kg<sup>-1</sup>, approximately 27-fold greater than that of the pristine one. The widened working voltage (1.1–2.1 V) and additional pseudocapacitance stemming from DmFc paved the way for the enhancement of the overall performance<sup>[45]</sup>. Recently, a new redox mediator, called tetrachlorohydroquinone (TCHQ), was used by Chen's group<sup>[46]</sup>. They found that TCHQ show impressive reversibility even with a large electrochemical window of 2.7

V. In addition, the theoretical calculation authorized that pyrrole N could catalyze the dehydrogenation reaction of TCHQ, providing distensible capacitance. The TCHQ-involved RE-SC delivered a specific capacity of 140 F g<sup>-1</sup> at 0.5 A g<sup>-1</sup>, 1.3 times higher than without the addition of TCHQ.

However, the characteristics of flammability, toxicity, and volatilization have limited the use of traditional organic electrolytes. Therefore, it is imperative to develop a cheap and environmentally friendly a novel organic electrolyte with low toxicity. Bio organic electrolyte may be a potential competitive organic electrolyte candidate owing to the advantages of degradability, low cost, and low toxicity. Chowdhury's team extracted pivalic acid (PA) from industrial wastes and bio-sources and further used it in the research of biological organic electrolyte. When PA was combined with ascorbic acid (AA) redox additives, the capacitor could provide an energy density of 15 Wh kg<sup>-1</sup> at a current density of 1 A g<sup>-1</sup>. A good coulombic efficiency of ~97% with a capacitance retention of ~72% could also be achieved after 10,000 charge-discharge cycles<sup>[47]</sup>. This work could widen the applications of bio-based redox electrolytes in electrochemical energy storage applications.

## 2.3 Ionic liquid redox electrolyte

Similar to organic electrolytes, ionic liquid electrolytes with a wide operating voltage window also couple with RE mediators to improve the electrochemical performance of SCs. Navalpotro et al. added p-benzoquinone (p-BQ) to N-butyl-N-methylpyrrolidinium bisimide as a redox electrolyte, and the results showed the capacity and energy density of 156 F g<sup>-1</sup> and 30 Wh kg<sup>-1</sup>, respectively, which were increased by 36% and 10% compared with those of SC without p-BQ<sup>[48]</sup>.

Besides being directly mixed with redox additives and ionic liquid electrolytes, redox-active groups can also be grafted onto the anion or cation of the ionic liquid<sup>[17]</sup>. For instance, two novel ionic liquid electrolytes containing ferrocene (Fc) imidazolium cations ([FcEmim][TFSI]) and bis(trifluoromethanesulfonyl)imide anions ([Emim][FcTFSI]) were designed by Xie, who investigated the effects of [FcEmim]<sup>+</sup> and [FcTFSI]<sup>-</sup> on the performance of SCs. The results affirmed the positive role of the Fc group in broadening the operating voltage (2.5 V) of the device. Consequently, the device delivers a high energy density of 13.2 Wh kg<sup>-1</sup>, which is an 83% increase over using unmodified ionic liquid<sup>[49]</sup>.

Inspired by Xie's work, You and coworkers studied the influence of Br and I substitution of ionic liquid anions on the electrochemical properties of the devices. In their work, 1-ethyl-3-methylimidazolium halide ([Emim]X) was prepared and used as an elec-

trolyte, where  $X = \text{Br}$  or  $\text{I}$ ,  $\text{Br}^-$ , and  $\text{I}^-$  act as redox-active ingredients to provide pseudocapacitance. The RE-SCs containing [Emim]-I and [Emim]-Br exhibited the energy densities of 175.6 and 161.2 Wh  $\text{kg}^{-1}$  at a current density of 1 A  $\text{g}^{-1}$ , respectively, closing to the level of Li ion batteries. Unfortunately, the high viscosity and low ionic conductivity due to the dual ionic liquids involvement led to poor power performance. The maximum power densities of [Emim]-I and [Emim]-Br containing device were only 4994.5 and 5267.0 W  $\text{kg}^{-1}$ , respectively<sup>[26]</sup>. Therefore, improving the overall performance of RE-SCs by modifying ionic liquids with redox species remains farfetched.

Table 1 summarizes the performance of some RE-SCs using aqueous, organic, and ionic liquid redox electrolytes. Though notable progress has been made, the low decomposition voltage of water (1.23 V) limits further development of aqueous RE-SCs. Meanwhile, the safety issues caused by the intrinsic nature of flammability, volatility, toxicity, and the high viscosity of organic electrolytes and ionic liquids hinder their application in areas requiring high safety factor and power output. Therefore, a novel design of redox additives or device configuration, which can broaden the stable working voltage of water as well as nonflammable and low-viscosity high-voltage supporting electrolyte, is urgently needed.

### 3 Self-discharge suppression strategy for RE-SC

Driven by Gibbs free energy, the charged SC undergoes spontaneous voltage drop under an open circuit, which, similar to Achilles heel, limits the wide application of the capacitor. The energy loss depending on the self-discharge rate varies for different types of

redox-active species used in the device. To greatly diminish the harmful effects of self-discharge, it is necessary to understand the mechanism of self-discharge formation first. Ohmic leakage, Faraday reaction, and charge redistribution are perceived as three widely accepted mechanisms of self-discharge<sup>[50]</sup>.

In general, charge redistribution is inevitable in SCs assembled via porous electrodes unless a special charging protocol is chosen<sup>[51]</sup> because the potential tested includes the charges located around the tip of the pores. After the external power supply is removed, some charges will move toward the pore depth driven by the concentration difference, causing the decline of measure voltage<sup>[52]</sup>. PSD affects the charge redistribution due to difference in the ion diffusion resistance. The resistance in small pores is bigger; therefore, the charge redistribution could also be adjusted via optimizing the PSD of an electrode.

Ohmic leakage is typically derived from an internal short circuit or parasitic redox reactions near the electrode/electrolyte interface. The relationship between the voltage and duration time can be described by the following equation<sup>[53]</sup>:

$$V = V_0 \exp\left(-\frac{t}{RC}\right) \quad (1)$$

where  $V$ ,  $V_0$ ,  $t$ , and  $RC$  represent the self-discharge voltage, initial voltage, self-discharge duration, and time constant on behalf of the resistance, respectively.

The Faraday reaction originates from the reactants (oxygen-functional groups on the carbon surface, redox mediator, and dissolved oxygen in the electrolyte) that can accept or lose electrons. According to the reactant concentration levels, it can be

**Table 1** Comparison of the electrochemical performance of the RE-involved SCs

Type	Electrolyte	Potential (V)	Capacitance	Energy density	Ref.
Aqueous redox electrolyte	$\text{H}_2\text{SO}_4 + \text{AgNO}_3$	1.0	82→248 F $\text{g}^{-1}$ (1 mA)	–	[21]
	$\text{Na}_2\text{SO}_4 + \text{K}_3\text{Fe}(\text{CN})_6$	1.6	93→475 mF $\text{cm}^{-2}$ (20 mA $\text{cm}^{-2}$ )	169 $\mu\text{Wh cm}^{-2}$	[33]
	$\text{KOH} + \text{K}_3\text{Fe}(\text{CN})_6$	0.6	152.9→207.7 F $\text{g}^{-1}$ (1 A $\text{g}^{-1}$ )	23.9 Wh $\text{kg}^{-1}$	[30]
	$\text{KOH} + \text{Na}_2\text{S}$	1.0	207→643 F $\text{g}^{-1}$ (1 A $\text{g}^{-1}$ )	12.6 Wh $\text{kg}^{-1}$	[34]
	$\text{H}_2\text{SO}_4 + \text{Na}_2\text{MoO}_4/\text{KI}$	1.0	27→470 F $\text{g}^{-1}$ (3 A $\text{g}^{-1}$ )	65.3 Wh $\text{kg}^{-1}$	[31]
	$\text{KOH} + \text{KI}$	1.0→1.6	–	7.1 Wh $\text{kg}^{-1}$ (3 A $\text{g}^{-1}$ )	[35]
	$\text{H}_2\text{SO}_4 + \text{HQ}$	1.0	220→412 F $\text{g}^{-1}$ (5 mA $\text{cm}^{-2}$ )	14 Wh $\text{kg}^{-1}$	[43]
	TEMPO	1.6	~30→~60 mAh $\text{g}^{-1}$ (0.5 A $\text{g}^{-1}$ )	51 Wh $\text{kg}^{-1}$	[39]
	$\text{KOH} + \text{KCl} + \text{TU}$	1.4	194→1154 mF $\text{cm}^{-2}$ (4 mA $\text{cm}^{-2}$ )	314.2 $\mu\text{Wh cm}^{-2}$	[42]
	Organic redox electrolyte	TBAP + DmFc	1.1→2.1	8.3→61.3 F $\text{g}^{-1}$ (1 A $\text{g}^{-1}$ )	36.76 Wh $\text{kg}^{-1}$
SBPBF <sub>4</sub> + TCHQ		2.7	~107.7→140 F $\text{g}^{-1}$ (0.5 A $\text{g}^{-1}$ )	35.7 Wh $\text{kg}^{-1}$	[46]
SP + AA		1.2	156→308 F $\text{g}^{-1}$ (1 A $\text{g}^{-1}$ )	15 Wh $\text{kg}^{-1}$	[47]
PYR <sub>14</sub> TFSI + p-BQ		3.0	114.7→156 F $\text{g}^{-1}$ (Pica) 23.3→70 F $\text{g}^{-1}$ (Vulcan) (5 mA $\text{cm}^{-2}$ )	30 Wh $\text{kg}^{-1}$ (Pica) 10.3 Wh $\text{kg}^{-1}$ (Vulcan)	[48]
Ionic liquid redox electrolyte	$\text{CH}_3\text{CN} + [\text{FcEMIm}][\text{NTf}_2]$	2.0	–	9 Wh $\text{kg}^{-1}$ (2 mA)	
	$\text{CH}_3\text{CN} + [\text{EMIm}][\text{FcNTf}_2]$	2.0	–	13.2 Wh $\text{kg}^{-1}$ (2 mA)	[49]
		2.5	–	23.7 Wh $\text{kg}^{-1}$ (2 mA)	

divided into activation- and diffusion-controlled reactions. An activation-controlled reaction is dominant when the concentration of impurities is high or the charging potential exceeds the decomposition potential of the solvent. The corresponding voltage after self-discharge can be expressed as the following formula<sup>[20]</sup>:

$$V = -\frac{RT}{\alpha F} \ln \frac{\alpha F i_0}{RT C} - \frac{RT}{\alpha F} \ln \left[ t + \frac{C\tau}{i_0} \right] \quad (2)$$

where  $R$ ,  $T$ ,  $\alpha$ ,  $F$ ,  $i_0$ ,  $C$ , and  $\tau$  represent the gas constant, temperature, transfer coefficient, Faraday constant, exchange current density, interfacial capacitance, and integration constant, respectively.

On the contrary, if the impurity concentration is low, they will require a long duration to pass through the electric double layer and to be oxidized or reduced. In this case, the diffusion-controlled reaction dominates the reaction process and can be remarked as follows<sup>[54]</sup>:

$$V = V_i - \frac{2zFAD^{1/2-1/2}c_0}{C} t^{1/2} \quad (3)$$

where  $V_i$ ,  $z$ ,  $D$ ,  $c_0$ , and  $A$  represent the initial voltage, charge of redox-active species, diffusion coefficient, initial concentration, and electrode area, respectively.

Notably, the aforementioned factors do not exist alone in a real situation. They may occur synchronously, thus causing complex self-discharge behavior. By combining them together, the real self-discharge process can be depicted as follows<sup>[55]</sup>:

$$V = V_0 \exp\left(-\frac{t}{RC}\right) - mt^{1/2} - a - b \ln \left[ t + \frac{CK}{i_0} \right] \quad (4)$$

where  $a$ ,  $b$ , and  $K$  represent the constants of the Faradic activation process and the integration constant, respectively.

Based on the self-discharge mechanism, various inhibition strategies have been proposed. Herein, we

mainly summarize the strategies from the separator, electrolyte, electrode modification, and device optimization. Moreover, we primarily focus on the influence of interaction between porous carbon and redox-active species on the shuttle effects of soluble redox mediators.

### 3.1 Separator modification

In general, the separator plays a dual role in insulating the negative electrode from the positive electrode and providing ion transport channels for the movement of electrolytic ions. Therefore, through reasonable design/modification of the separator, including ion selectivity modification, pore size optimization, and polarity modulation, it can play a role in inhibiting ion shuttle for controlling self-discharge<sup>[50]</sup>.

The suppression of capacitor self-discharge can be achieved by using ion exchange membranes (IEM)<sup>[56]</sup>. For example, Lee et al. used a cation exchange membrane instead of a porous hydrophilic polytetrafluoroethylene separator (ONP) to inhibit the shuttle crossing of  $[\text{Fe}(\text{CN})_6]^{3-}/[\text{Fe}(\text{CN})_6]^{4-}$  couples. As shown in Fig. 5a, the addition of  $\text{K}_3[\text{Fe}(\text{CN})_6]$  significantly accelerated the self-discharge of the capacitor; however, when IEM was used, the self-discharge rate was significantly reduced. The open circuit voltage (OCV) maintained over 75% of its initial voltage after 10 h while that of the device using ONP almost reduced to 0 V under 1 h<sup>[57]</sup>. Unfortunately, the high cost of IEM has deterred many studies.

A polyacrylonitrile coated by sodium dodecyl benzene sulfonate (PAN@SDBS) nanofiber membrane was fabricated and further used as a separator for SC.  $\text{Na}^+$  can be released in the KOH electrolyte, and this process impart a negative charge to the separator. In this case, the anions on the positive electrode are electrostatically repelled by the negative charges on the separator, thereby their migration is

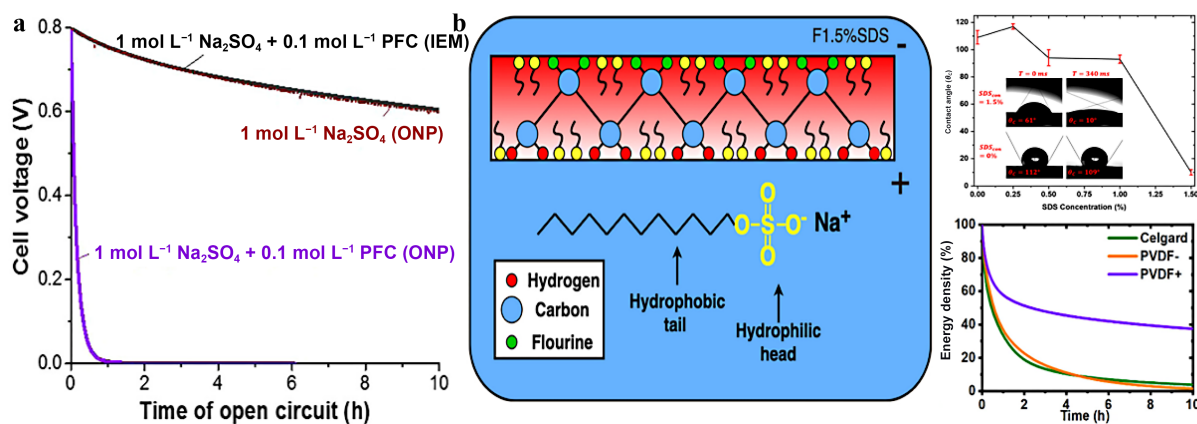


**Figure 5** (a) Time dependence of the open circuit voltage (OCV) for 1 mol L<sup>-1</sup> Na<sub>2</sub>SO<sub>4</sub> with and without 0.1 mol L<sup>-1</sup> PFC. Data are provided for the use of a porous separator (ONP) and an ion exchange membrane (IEM)<sup>[57]</sup>. Copyright 2016, American Chemical Society. (b) Illustration of the possible orientation of the SDS molecules in the hybrids and the contact angle and energy change in different systems<sup>[59]</sup>. Copyright 2023, Wiley-VCH.



suppressed<sup>[58]</sup>. The voltage remains at 0.58 V after 12,000 s when the PAN@SDBS membrane is used, while it is higher than those of the commercial separator-used (0.38 V) and pure PAN-used (0.34 V) devices.

Based on a similar principle, Buxton et al. induced polarity of the separator by tailoring the amount of sodium dodecyl sulfate (SDS) in a polyvinylidene fluoride (PVDF) nanofiber membrane<sup>[59]</sup>. As displayed in Fig. 5b, the dosage of SDS affects the surface hydrophilicity of the separator, which is an important index for aqueous-based SCs. This polarized separator successfully suppresses self-discharge by dropping the initial voltage of 1.6 to 1 V after 10 h, compared to 0.3 V for the nonpolarized separator with the energy retention of 37% and 4%, respectively.

The shuttle of polysulfides has been reportedly suppressed in lithium-sulfur batteries by adjusting the PSD of separators<sup>[60]</sup>. Thus, we believe that the self-discharge of SC can also be suppressed by a similar approach. In general, when the size of the hole in the separator is smaller than the redox mediator molecules, they will be completely blocked from passing. Liang et al. assembled graphdiyne oxide/polyvinyl alcohol (GDYO/PVA) membrane to alleviate serious self-discharge by benefiting from intrinsic selective nanopores of GDYO. The smaller PSD of GDYO (ca. 0.38 nm) than those of  $I^-$  (0.39 nm) and  $I_3^-$  (0.63 nm) plays a critical role in inhibiting the diffusion of redox-active species. In addition, the hydrogen bonding between the GDYO and PVA molecules also plays an important role in inhibiting ion diffusion. Consequently, the SC with GDYO/PVA separator takes 37,160 s to drop the voltage from 1 to 0.3 V, about 153 times longer than the device with commercially available PP film<sup>[61]</sup>.

Although self-discharge can be effectively suppressed by membrane modification, this method could significantly increase the ion diffusion resistance and limit the ion transport, thereby reducing the power characteristics and rate capability of the SCs.

### 3.2 Electrolyte modulation

Similar to separator modification, the core purpose of electrolyte regulation is to suppress the irreversible shuttle of ions. By choosing a special redox electrolyte or adjusting its molecular structure, an electrode-electrolyte interface emerges with different strengths; consequently, the self-discharge can be suppressed. In this section, we summarize several common strategies to suppress self-discharge by regulating the electrolyte.

#### 3.2.1 Solid complexation

Li's study found that when  $CuSO_4$  was used as the redox medium instead of BQ, insoluble Cu formed

on the negative electrode surface during charging, thereby inhibiting the shuttle of redox-active species. In the OCV-time curve, the capacitor with the  $CuSO_4/H_2SO_4$  electrolyte has a considerably slower self-discharge process than the capacitor with the BQ/ $H_2SO_4$  electrolyte. It requires 7727 s for the  $CuSO_4/H_2SO_4$  system and 1462 s for the BQ/ $H_2SO_4$  device to decrease from 0.8 to 0.3 V, which indicates an effective suppression of self-discharge (Fig. 6a)<sup>[62]</sup>. Although the deposition of Cu on the negative electrode serves to suppress self-discharge, insoluble Cu inevitably leads to the pore-clogging effect and deterioration of cycling stability, which can cause serious capacity degradation.

Inspired by the interesting work mentioned above, a new strategy based on the concept of solid complexation was proposed by Stucky and coworkers through the research of viologen molecules and bromide<sup>[63-65]</sup>. They discovered that the branched chains in viologen molecules played an important role in tuning the overall performance of viologen/bromide-involved hybrid electrolytes. For example, when coupling heptyl viologen (HV) with KBr, an energy density of 11 Wh  $kg^{-1}$  at a specific power of 122 W  $kg^{-1}$  along with a slow self-discharge rate can be achieved. When the HV was replaced by methyl viologen (MV), a higher specific energy of 14 Wh  $kg^{-1}$  and fast self-discharge were found, indicating that the electrochemical performance varies as a function of the chemical and molecular structures of viologen<sup>[63]</sup>. To deeply understand the reason of the self-discharge, they investigated the behavior of viologen molecules and bromides ( $Br^-/Br_3^-$ ) with different branched chains. As shown in Fig. 6b, during charging, the viologen ( $V^{2+}$ ) and the tribromine anion ( $Br_3^-$ ) formed an insoluble complex  $[V^{2+} \cdot 2Br_3^-]$  at the positive electrode, while a solid complex  $[V^+ \cdot Br^-]$  was formed at the negative electrode, leading to the deposition of charged products on the porous carbon electrode. When discharging, the opposite process occurs, and the solid complexes dissolve from the electrode surface into the native electrolyte. The solid complexes generated during the charging process can suppress the diffusion of redox-active couples in the charged state to prevent any side reactions and self-discharge. Consequently, the assembled device delivers a high specific energy of 48.5 Wh  $kg^{-1}$  along with amazing stability, maintaining 97% of energy after 10,000 cycles at a current density of 2.5 A  $g^{-1}$ <sup>[64]</sup>.

Subsequently, they brought tetrabutylammonium cation ( $TBA^+$ ) to the bromide cathode electrolyte to induce the formation of reversible solid-state complexes of  $Br_2/Br_3^-$ <sup>[65]</sup>. Since these solid-state complexes can be confined in the pores of electrodes, this approach can be perceived as a "killing two birds with one stone" strategy that can achieve the dual

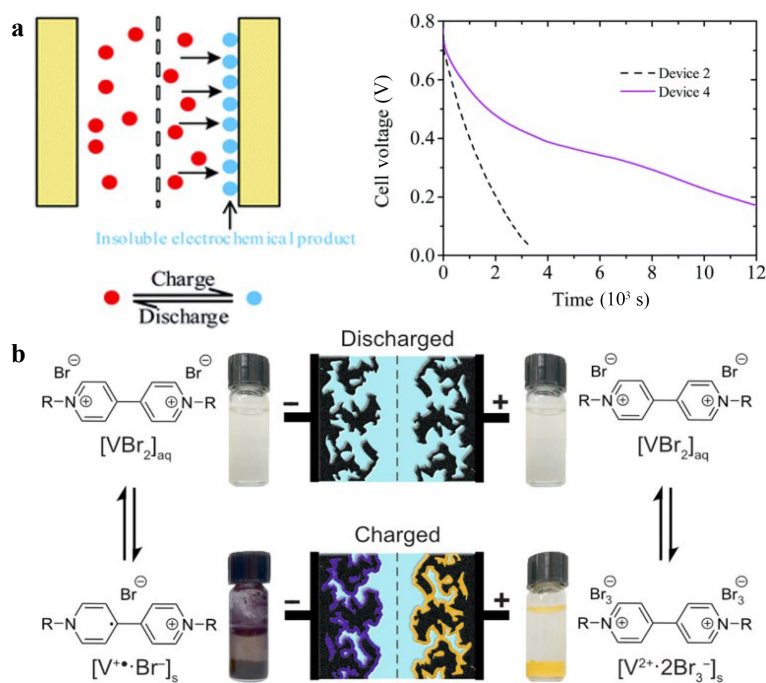


**Figure 6** (a) Conversion of Cu<sup>2+</sup> into insoluble species during the charging process and the self-discharge curves<sup>[62]</sup>. Copyright 2008, Royal Society of Chemistry. (b) Mechanism of reversible solid complex formation based on viologen and bromine during charging/discharging<sup>[64]</sup>. Copyright 2016, American Chemical Society.

purpose of high redox activity and high stability. Based on this mechanism, the as-fabricated RE-SC delivers high energy density (64 Wh kg<sup>-1</sup>), impressive power density (3 kW kg<sup>-1</sup>), long cycling life, and slow self-discharge rate.

### 3.2.2 Molecular structure control

As mentioned in Section 2.3, by reasonably designing the molecular structure of the ionic liquid, a stable passivation layer appears during charging, leading to a low self-discharge rate. However, the limited ion/electron transport caused by the passivation layer deteriorates the power output and cycling life<sup>[49]</sup>. To address this problem, Mourad designed a biredox ionic liquid where the anion was functionalized with AQ and the cation was modified with TEMPO moieties<sup>[11]</sup>. The ionization of redox groups contributes to the increased density of the redox groups in the liquid state approaching the bulk density of redox solids, thereby resulting in higher capacity and faster redox kinetics than surface-immobilized redox-active species. Interestingly, the reduced/oxidized species are doubly charged and can be electroadsorbed at the charged electrode, thereby reducing free diffusion and self-discharge. The leakage current in the biredox ionic liquid involved electrolyte is between 30 and 40 μA F<sup>-1</sup>V<sup>-1</sup>, two or three times lower than the cell with a conventional electrolyte (100 μA F<sup>-1</sup>V<sup>-1</sup>).

### 3.2.3 Electric field induction

The ion diffusion can also be retarded by introduc-

ing extra electrorheological molecules, which could affect the viscosity when an electric field is applied<sup>[50]</sup>. Precisely, when an electric field is applied, liquid crystal molecules undergo directional alignment, leading to a significant increase in the fluid viscosity near the electrode surface.

Xia et al. introduced the nematic liquid crystal 4-*n*-pentyl-4'-cyanobiphenyl (5CB) to the TEMABF<sub>4</sub>/acetonitrile electrolyte to probe its effect on the suppression of self-discharge<sup>[55]</sup>. The principle of the function of 5CB is shown in Figs. 7a and 7b. Upon charging, the 5CB molecules undergo rearrangement to form an ordered arrangement that is perpendicular to the electrode surface due to the electrorheological effect, resulting in higher viscosity near the electrode/electrolyte interface. Owing to the well-tuned fluid rheological properties of the electrolyte, the diffusion of ions and redox substances in the electrolyte could be hindered, resulting in slower self-discharge rate. Notably, the 5CB molecules would be turned into a disordered state, and the electrorheological effect would disappear during the discharge process. Accordingly, it takes 16.5 h for the SC containing 5CB to drop from 2.0 to 1.5 V, almost seven times longer than that of the one without 5CB (Fig. 7c). Moreover, the leakage current of the capacitor with 5CB is only 2.2 μA, substantially smaller than that of the other one (12 μA). A similar effect can also be found when the supporting electrolyte is altered as an aqueous electrolyte<sup>[66]</sup>.

In addition to using a single species to inhibit self-discharge, multi-species hybridization is another

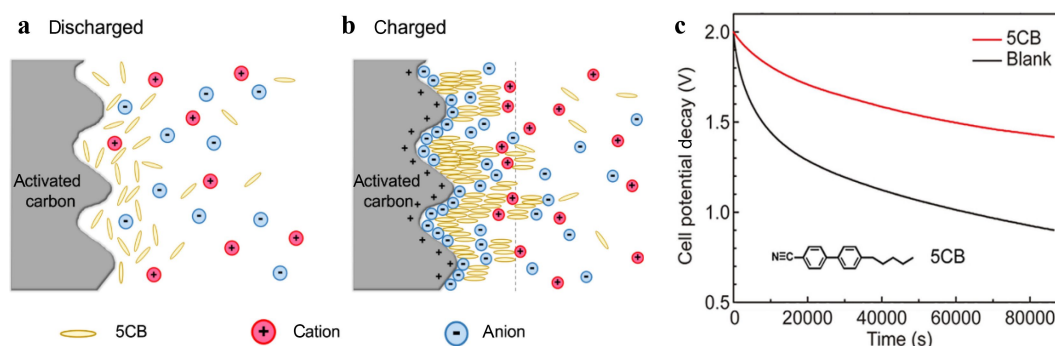


**Figure 7** (a) Illustration of the electrode–electrolyte interface with 5CB added to the electrolyte. In the discharged state, cations, anions, and 5CB molecules in the electrolyte are uniformly distributed. (b) When the electrode is charged, the electric field near the electrode surface causes the 5CB molecules to align toward the electric field and enhances the flow viscosity. (c) Potential–time plots with and without the 5CB<sup>[55]</sup>. Copyright 2018, Elsevier.

effective approach to improve self-discharge performance. For example, a new hybrid liquid crystal E7 composed of 5CB (51%), 7CB (21%), 8OCB (16%), and 5CT (12%) monomers was prepared by Su et al. and further used as an additive to the electrolyte to suppress the self-discharge of activated carbon-based SC<sup>[67]</sup>. In this mixture, 7CB, 8OCB, and CT are 4-*n*-heptyl-4′-cyanobiphenyl, 4-octyloxy-4′-cyanobiphenyl, and cyanotriphenyl, respectively. The OCV of the device with E7 decreased from 3 to 1.4 V after 24 h. The leakage current was also reduced from 10 to 2.2  $\mu\text{A}$  due to the presence of E7. Even at 60°C, E7-added electrolytes still exhibited a remarkable suppression of self-discharge, thus providing a useful strategy to improve the performance of SCs.

In addition, the electric field can also be affected by the high concentration of the electrolyte via changing the electron transfer between the electrode and electrolyte. When 14 mol L<sup>-1</sup> instead of 1 mol L<sup>-1</sup> LiCl was adopted as an electrolyte, 40 times longer time was needed to drop the OCV to the same voltage<sup>[68]</sup>. They found that the self-discharge mechanism turns from an activation-controlled to a diffusion-controlled faradaic reaction due to the increased number of hydration clusters and decreased number of free water molecules, which leads to a reduced rate of electron transfer.

### 3.2.4 Gel/solid-state electrolyte

A proven efficacious method to alleviate self-discharge involves using solid or gel electrolytes. The voltage dropped rapidly from 1 to 0.5 V in 1720 s for the RE-SC using an aqueous CuCl<sub>2</sub>/H<sub>2</sub>SO<sub>4</sub> electrolyte. In contrast, a substantially slower voltage decay was observed when the PVA/CuCl<sub>2</sub>/H<sub>2</sub>SO<sub>4</sub> gel electrolyte was adopted. It takes 18,465 s to drop from 1 to 0.5 V, which is 10 times longer than the voltage change in the aqueous one<sup>[69]</sup>. However, low ionic conductivity leads to insufficient power density. To solve this problem, Hashmi et al. immobilized KI and 1-ethyl-3-methylimidazolium bis(trifluo-

romethylsulfonyl)imide into poly(vinylidene fluoride-co-hexafluoropropylene) to prepare a gel electrolyte with high ionic conductivity. The assembled all-solid-state capacitor exhibited excellent rate performance and cycle stability while maintaining a slow self-discharge rate<sup>[70]</sup>.

Based on a similar concept to gel electrolytes, solid-state electrolytes can reduce the self-discharge rate by weakening the ion transport rate. Wang et al. proposed a “playing mud pies” strategy to fabricate bentonite clay@ionic liquid-based solid-state electrolyte (BISE). The BISE-based SC displays an extremely low self-discharge rate with an OCV drop of only 28.9% within 60 h, which is significantly better than that of conventional SC (40.1%@12 h). Moreover, even at 75°C, the device can present a low voltage decline of 40% within 12 h and can stably provide a high voltage of >1.5 V<sup>[71]</sup>. The confinement effect of Si–O bonds of the clay is responsible for suppressing the shuttle effect of Fe ions and promoting selective penetration of electrolyte anions.

### 3.3 Electrode modification

As an important part of RE-SCs, the basic characteristics (pore structure and surface polarity) of electrode materials not only affect the quantity of energy storage processes but also have a considerable impact on the quality of their energy storage capability (cycling stability and self-discharge behavior). The works of separator modification and electrolyte regulation to directly or indirectly inhibit self-discharge prove that strengthening the interaction between electrolytic ions and the electrode interface is helpful in inhibiting the occurrence of self-discharge and weakening the side effects of self-discharge on the RE-SC system. In this part, we focus on the influence of the possible interaction between the redox-active species and the typical nature of the electrode materials, including the pore structure and surface functional groups, on the construction of a strong elec-

trode–electrolyte interface to inhibit the ion shuttle.

### 3.3.1 Pore structure

The intrinsic pore properties, such as the size and shape of carbon-based electrodes, play an important role in ion adsorption and diffusion. To investigate the influence of PSD on charge redistribution, Wang et al. proposed a novel controlled current-source-based ladder equivalent circuit model (ECM) expressed in Fig. 8a<sup>[72]</sup>. The ECM has tree branches representing the macro, meso, and micropores. The resistances in each branch stand for the electrolyte, electrode, and self-discharge resistances, respectively. Based on the experimental data and simulation results, the percent relative error of the proposed ECM is within 0.8%, confirming the important influence of PSD on the self-discharge process.

Pore shape is another important factor affecting ion transport and diffusion. To analyze the impact of pore shape structure on self-discharge, stacked carbon nanosheets (S-CNS), double-layer carbon nanosheets (DL-CNS) and flower-like carbon nanosheets (FL-CNS) with similar pore diameters but different pore shape structures were prepared<sup>[73]</sup>. As expected, due to the different pore structures and correspondingly different ion transport resistances,

the rate performances increased from S-CNS, FL-CNS to DL-CNS SCs (Fig. 8b). However, for the pore shape with fast ion transport, it is difficult to maintain higher energy at the OCV due to the rapid ion diffusion; therefore, the voltage drop is more pronounced. As presented in Fig. 8b, the OCV of S-CNS-, FL-CNS-, and DL-CNS-based SC drops from 2 V to 0.99, 0.74, and 0.53 V after 24 h, respectively. Simulations of the OCV decays indicate that the self-discharge processes of the three carbon materials were jointly controlled by a diffusion-controlled process and an ohmic leakage process. Therein, the diffusion-controlled process corresponding to the faster self-discharge rate dominates in the first several hours, while an ohmic leakage process is responsible for the subsequent slower self-discharge. The results of this study indicate that balancing the rate performance and energy loss caused by self-discharge must be greatly emphasized.

Regarding the effect of pore diameter on self-discharge behavior, Zhang et al. conducted related research by using multi-walled carbon nanotubes (MWCNTs) with different diameters of 20, 30, and 50 nm as the research object. The self-discharge rate was found to reduce with the decreasing diameter of MWCNTs due to the augmented diffusion resistance.

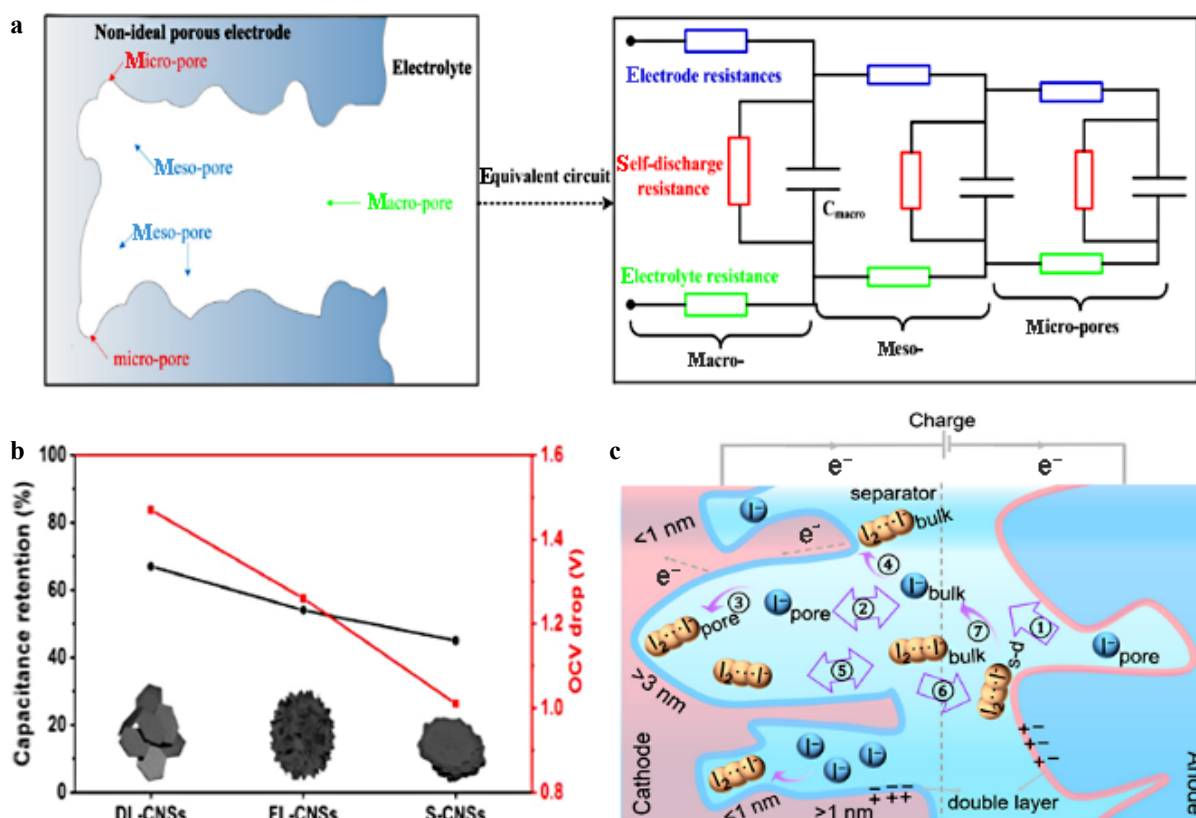


**Figure 8** (a) Equivalent circuit model (ECM) based on the macro, meso, and micropore structures<sup>[72]</sup>. Copyright 2020, Elsevier. (b) Pore structures as a function of specific capacity and open-circuit voltage<sup>[73]</sup>. Copyright 2021, Elsevier. (c) Illustration of the charge storage mechanism involving multiple physical transfer processes in porous carbon electrodes and native solutions. Iodide is used as a redox mediator. Self-discharge is denoted by the abbreviation “s-d”<sup>[76]</sup>. Copyright 2021, American Chemical Society.

Specifically, the degree of OCV decay always increases with the pore diameter regardless of the adopted initial voltage<sup>[74]</sup>. Lee et al. found that after 12 h under an open circuit, the devices assembled by electrodes with pore diameters under 1 nm (i.e., 0.7 and 0.8 nm) had a higher charge retention rate of 87% than 69% for the one with pore diameters exceeding 1 nm (1.1 nm) due to the strong adsorption behavior of <1 nm micropores on the redox electrolyte ions I<sup>-</sup> and I<sub>3</sub><sup>-</sup><sup>[75]</sup>. Zhao et al. reported an investigation of a range of commercial and laboratory-synthesized carbon materials for RE-SCs with KI as a demo focusing on the fundamental analysis of how to optimize a specific carbon for RE-SC<sup>[76]</sup>. In their work, the fastest rates are typically observed with pore-sizes >1 nm, while slow self-discharge requires pores <1 nm (Fig. 8c). Thus, carbon with substantial hierarchy in pore size, including smaller, <0.8 nm pores and larger, 1.1–3 nm pores, showed the best overall performance, illustrating key design principles.

By using density functional theory calculations, Schweizer et al. studied the interaction between the pore diameter of the carbon-based electrode material and the electrolyte. In this work, CNTs with different diameters ranging from 6.7 to 13.5 Å were chosen as a model to study the effect of pore diameter on ionic interactions by confining the cation TEA inside the CNTs. Combining the experimentally determined pore confinement effects and calculated interaction energies, it was found that pore diameter notably affects the interaction with the electrolyte. After complete geometric optimization, the interaction energies were calculated. For the cationic TEA system, the interaction energy ranges from -33.5 to -228.7 kJ mol<sup>-1</sup><sup>[77]</sup>. CNTs (7,7) with a diameter of 9.5 Å showed the strongest interaction with TEA. The actual normalized capacitance-average pore diameter relationship exhibited the highest capacitance at an average pore diameter of about 8.3 Å, which tended to shift toward a larger value compared to the simulated calculated data. This is possibly because CNTs are a simplified model with two open ends and a highly regular structure compared to the real cavity in the electrode. The results indicated that an optimal pore size exists for limiting ions, and the more the pore size fits the ion size, the stronger the interaction, in which case the self-discharge behavior will be suppressed effectively.

### 3.3.2 Surface functionalization

Carbon electrodes are nonpolar; thus, they exhibit a weak affinity for redox mediators, which causes a large fraction of redox mediators to move away from the solid-liquid interface and shuttle between the cathode and anode<sup>[78]</sup>. The functional groups on carbon electrodes acting as a bridge between the elec-

trode and redox mediator can effectively enhance their interaction. Furthermore, functionalization can also contribute to fast charge transfer, provide additional redox-active sites, and accelerate the redox reactions involving some ions. More importantly, some redox molecules can be anchored to the electrode through the functional groups on the carbon electrode surface, which can inhibit their shuttling and thus suppress capacitor self-discharge<sup>[79]</sup>.

Zhai et al. reported a simple and effective solvothermal method to functionalize ethylenediamine (EDA) on porous carbon to form surface-functionalized carbon materials modified with basic groups (-NH<sub>2</sub>/-NH-)<sup>[41]</sup>. This functionalized porous carbon was used as electrodes to construct RE-SCs with p-phenylenediamine (PPD) + KOH and HQ + H<sub>2</sub>SO<sub>4</sub> redox electrolytes, respectively. As shown in Fig. 9a, PPD and HQ can be attached to the amino group (-NH<sub>2</sub>/-NH-) of the EDA-functionalized porous carbon through hydrogen bonding, resulting in energy densities of up to 8.3 and 8.8 Wh kg<sup>-1</sup> in the electrolytic systems of PPD and HQ, respectively. This hydrogen bonding between functional groups leads to enhanced electrode-electrolyte interface interactions, which in turn favors considerably higher cycling stability of the capacitors. After 10,000 cycles at 4 A g<sup>-1</sup>, the stability of PPD and HQ can be maintained at 94% and 97%, respectively.

Isikli et al. covalently grafted p-BQ onto the surface of a carbon electrode via the Friedel-Crafts reaction with FeCl<sub>3</sub> as a catalyst and investigated its bioelectrochemical properties as a supercapacitor<sup>[83]</sup>. Shul et al. chemically grafted AQ molecules onto the negative surface of carbon black electrodes in the same way and studied the self-discharge of redox mediator<sup>[80]</sup>. Compared with the capacitor adding quinone in the electrolyte directly, the self-discharge of the RE-SC based on chemically grafted redox molecules was significantly slower, as shown in Fig. 9b. In the fully charged capacitors, when the voltage drops by 50%, the device assembled by functionalized electrode takes 6 h, ten times longer than the other device. The redox mediator migration is severely restricted due to the grafting of AQ molecules on the negative electrode.

Cao et al. introduced the oxygen-functional group to electrochemically activated carbon nanotubes (EACNTs). The oxygen-containing functional groups on the carbon electrode surface were anchored to the K-EACNTs through strong interactions of the redox mediator with [Fe(CN)<sub>6</sub>]<sup>3-</sup>/[Fe(CN)<sub>6</sub>]<sup>4-</sup><sup>[81]</sup>. As shown in Fig. 9c, this enables an effective confinement of redox ions around the carbon electrode and enhances the electron transfer between the electrode and redox electrolyte. Owing to this interface, this system exhibits a low self-discharge rate and no decay in specific capacitance

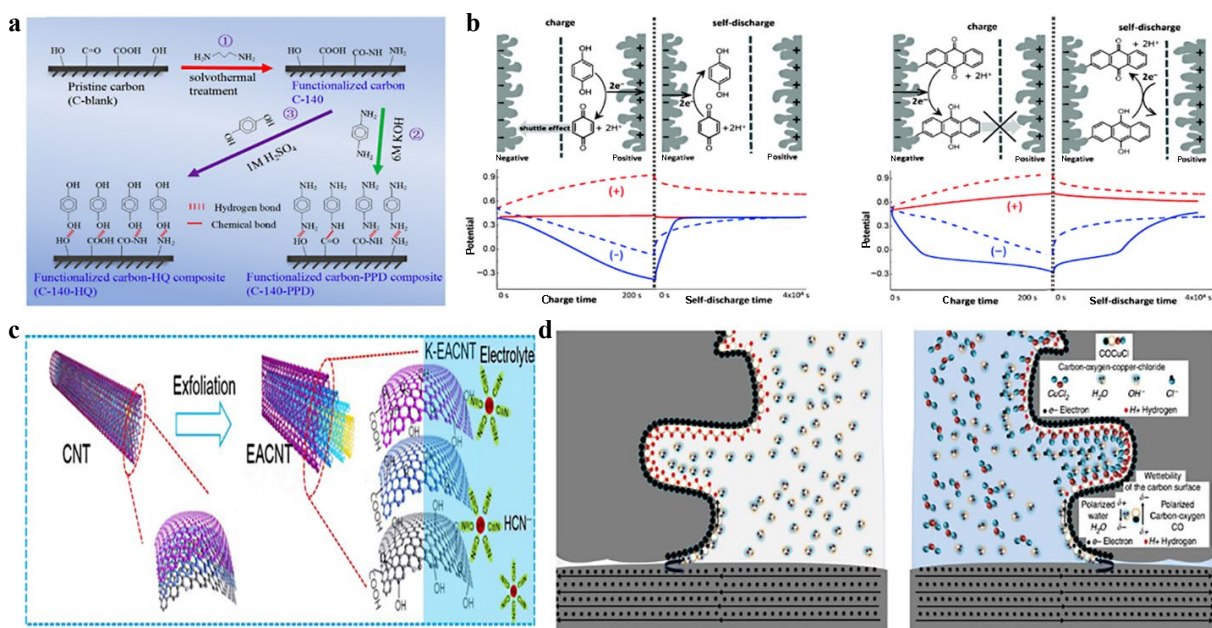


**Figure 9** (a) Schematic representation of the surface functionalization of porous carbon by solvothermal method and interaction with redox additives of phenylenediamine (PPD) and hydroquinone (HQ) on the carbon surface<sup>[41]</sup>. Copyright 2019, Elsevier. (b) Schematic representation of electrochemical reactions occurring during charging and self-discharge of supercapacitors containing HQ- and AQ-redox substances and the corresponding potential distributions for each electrode and for those without redox substances<sup>[80]</sup>. Copyright 2016, Royal Society of Chemistry. (c) Schematic diagram of electrochemically activated carbon anchoring redox mediator [Fe(CN)<sub>6</sub>]<sup>3-</sup> by oxygen-containing functional groups<sup>[81]</sup>. Copyright 2021, Elsevier. (d) Schematic diagram before and after the CuCl layer formation on the surface near the pores<sup>[82]</sup>. Copyright 2013, Springer Nature.

after 32 h in the open-circuit state, thus achieving suppressed self-discharge. As shown in Fig. 9d, the oxygen-functional groups (C=O) can also be used to adsorb Cu<sup>2+</sup> to form a CuCl layer on the electrode surface to inhibit ion diffusion and accelerate charge transfer, leading to enhanced capacitance and cycle lifetime<sup>[82]</sup>.

This oxygen-functional-group-induced chemical grafting can also be extended to other metal compounds. For example, by combining the strategies of space confinement and chemical bridging, Sheng et al. constructed an RE-SC with ultra-high power density (79.1 kW kg<sup>-1</sup>) and ultra-long cycling life (100% capacitance retention after 20,000 cycles), wherein [Fe(CN)<sub>6</sub>]<sup>3-</sup>-grafted honeycomb carbon framework and Na<sub>2</sub>SO<sub>4</sub> were used as electrode and electrolyte<sup>[84]</sup>.

### 3.4 System optimization

In addition to the modifications of the separator, electrolyte, and electrode, system design is another choice for modulating ions. Herein, special device designs, including adding a functional barrier layer and asymmetric design using two different electrodes and/or electrolytes, are discussed.

#### 3.4.1 Addition of a barrier layer

The application of a barrier layer with an insulating material on the electrode surface is another good strategy to suppress self-discharge, wherein the

barrier layer increases the distance between ionic and electronic charges, hinders electron transfer, and mitigates leakage currents. Tevi et al. reduced the leakage currents by electrodepositing a thin layer of polyphenylene oxide (PPO) as a barrier layer on a glassy carbon substrate<sup>[85]</sup>. Figures 10a and 10b illustrate the electrode–electrolyte interface and the corresponding equivalent electrical circuits with and without the PPO layer. The OVC-time plots depicted in Fig. 10c demonstrate the positive effect of the PPO layer on suppressing the self-discharge. The application of the PPO layer reduced the leakage current by 78%. However, the specific capacitance was decreased by 56% when the blocking layer was applied. Subsequently, they systematically studied the effect of the barrier layer thickness on self-discharge and specific energy via a mathematical model composed of simple quantum mechanical and electrochemical phenomena occurring during self-discharge. Recently, Hamedi et al. found that a constant parallel resistance cannot accurately model the nonlinear characteristic of the self-discharge behavior. Therefore, they improved Tevi's model and found that the new time-varying model is more suitable for the fitting analysis of the self-discharge curves<sup>[86]</sup>.

#### 3.4.2 Asymmetric design

In the RE-SCs, the redox reaction generally occurs at one electrode; thus, the total capacitance of such SCs

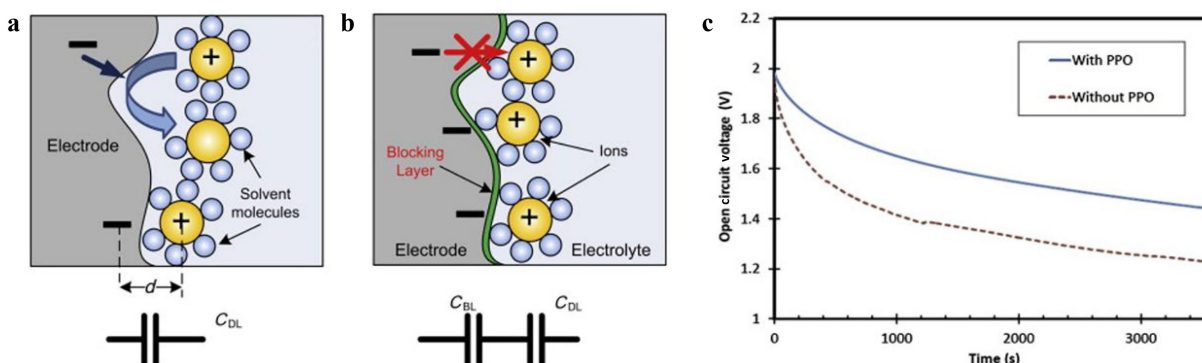


**Figure 10** Schematic diagram of the electrode–electrolyte interface in supercapacitors (SCs) and their equivalent electrical circuits (a) without and (b) with a blocking layer. (c) Open circuit voltage (OCV)–time plots with and without the polyphenylene oxide (PPO) blocking layer<sup>[85]</sup>. Copyright 2013, Elsevier.

will be limited by the low-capacitance electrode. Therefore, a proper asymmetric design to balance the capacity between two electrodes is of great importance to construct a high-performance device with high total capacitance, long lifetime, and low self-discharge. In this section, the aforementioned asymmetric design contains two meanings: (i) asymmetric devices based on different positive and negative electrode materials and (ii) asymmetric devices based on different structures of positive and negative electrolytes.

Frackowiak et al. reported a carbon-based asymmetric SC that integrates 1 mol L<sup>-1</sup> KI solution and 1 mol L<sup>-1</sup> VOSO<sub>4</sub> solution as an electrolyte, separated by a Nafion membrane. The supercapacitor achieved a high specific energy of approximately 20 Wh kg<sup>-1</sup> with a maximum power density of 2 kW kg<sup>-1</sup><sup>[87]</sup>. Inspired by this work, Lee et al. assembled an asymmetric SC based on an aqueous electrolyte containing SnSO<sub>4</sub> and VOSO<sub>4</sub> with activated carbon<sup>[88]</sup>. Benefiting from the unique synergy of concurrent electric-double layer formation, reversible tin redox reactions, three-step redox reactions of vanadium, and the involvement of IEM, the asymmetric device exhibited a broad and stable window up to 1.4 V with a high specific energy of 75.4 Wh kg<sup>-1</sup> as well as a long cycling life and low level of self-discharge rate. Particularly, after 10 h of OCV measurement, the initial voltage dropped by approximately 17%, which is only half that of the device operated in 1 mol L<sup>-1</sup> H<sub>2</sub>SO<sub>4</sub>.

In general, the coupling of an electrode and a redox additive possesses weak electrode/RE interaction and weak adsorption of redox moieties on the electrode, which is responsible for the low-capacity contribution and fast self-discharge. To mitigate these shortcomings in RE-SCs, a synergistic interface-assisted electrode–electrolyte coupling strategy was proposed<sup>[23]</sup>. In this work, Fe(CN)<sub>6</sub><sup>4-</sup> groups are grafted on the surface of the Co<sub>3</sub>O<sub>4</sub> electrode via the formation of Co–N bonds, creating a synergistic interface between the electrode and redox mediator,

which favors efficient electron transfer during the charge/discharge process. The unique interface can also introduce dipole–dipole interaction for the greatly enhanced adsorption of redox-active molecules. Consequently, the HCO-PFC//FG cell, retaining 38% of full energy after 4.7 h, exhibited significantly reduced self-discharge than the CO-PFC//FG cell, reserving only 24% of full energy after 1.5 h.

For a more intuitive understanding of the effects of different self-discharge suppression strategies, Table 2 is prepared, from which one can find that all the aforementioned strategies could improve the voltage retention under the OCV and superior performance is desired for a high-performance RE-SC.

## 4 Conclusion and outlook

The construction of carbon-based RE-SCs by replacing the inert electrolyte with a redox-active electrolyte has stormed academic research due to numerous significant advantages of achieving high energy density and impressive power output simultaneously in one device, thereby filling the gap between conventional SCs and secondary batteries. In the past few years, considerable endeavors have been made regarding the exploration of new types of redox-active species, and substantial progress has been achieved, especially in the enhancement of energy density. However, compared with the conventional electrical double-layer capacitors, the research on the RE-SC systems is still at an infant stage; more extensive and thorough investigations are desired for their applications. Therefore, more attention should be paid to alleviating the severe self-discharge concern in RE-SCs.

In this review, we summarize the recent progress of RE-SCs, starting from the redox-active mediators suitable for different supporting electrolytes, followed by the self-discharge suppression strategies recently used from the aspects of modulation of the separator, electrolyte, electrode, and system construc-

**Table 2** Self-discharge suppression effect of different strategies

Type	Strategy	Electrolyte	OCV decay	Ref.
Separator modification	IEM replace ONP	$\text{Na}_2\text{SO}_4 + \text{K}_3\text{Fe}(\text{CN})_6$	0 (10 h) $\leftarrow$ 0.8 $\rightarrow$ 0.6 V (10 h)	[57]
	Polarity modulation	KOH	0.34 (~3.33 h) $\leftarrow$ 1.0 $\rightarrow$ 0.58 V (~3.33 h))	[58]
		$\text{Na}_2\text{SO}_4$	0.4 (10 h) $\leftarrow$ 1.6 $\rightarrow$ 1.0 V (10 h)	[59]
	Pore size optimization	$\text{H}_2\text{SO}_4 + \text{KI}$	0.3 (~7.54 h) $\leftarrow$ 1.0 $\rightarrow$ 0.3 V (~10.32 h))	[61]
	Solid complexation	$\text{H}_2\text{SO}_4 + \text{CuSO}_4$	0.3 (~0.41 h) $\leftarrow$ 0.8 $\rightarrow$ 0.3 V (~2.15 h)	[62]
Electrolyte modulation	Molecular structure control	$\text{EVBr}_2 + \text{TBABr} + \text{NaBr}$	$\leftarrow$ 1.35 $\rightarrow$ 1.13 V (6 h)	[65]
		Biredox ionic liquid	1.4 (~45 h) $\leftarrow$ 2.8 $\rightarrow$ 1.4 V (~50 h)	[11]
	Electric field induction	5CB + TEMABF <sub>4</sub>	0.9 (24 h) $\leftarrow$ 2.0 $\rightarrow$ 1.42 V (24 h)	[55]
		E7 + TEMABF <sub>4</sub>	1.1 (24 h) $\leftarrow$ 3.0 $\rightarrow$ 1.4 V (24 h)	[67]
		PVA + CuCl <sub>2</sub> + H <sub>2</sub> SO <sub>4</sub>	0.5 (~0.51 h) $\leftarrow$ 1.0 $\rightarrow$ 0.5 V (~5.13 h)	[69]
Electrode modification	Gel/solid-state electrolyte	PVDF-HFP + EMITFSI + KI	$\sim$ 0.8 (16 h) $\leftarrow$ 2.75 $\rightarrow$ $\sim$ 0.95 V (16 h)	[70]
		BISE	$\sim$ 1.78 (12 h) $\leftarrow$ 3.0 $\rightarrow$ $\sim$ 2.13 V (60 h)	[71]
	Pore structure	TEABF <sub>4</sub> + PC	0.53 (24 h) $\leftarrow$ 2.0 $\rightarrow$ 0.99 V (24 h)	[73]
		MeEt <sub>3</sub> NBF <sub>4</sub> + AN	0.18 (24 h) $\leftarrow$ 1.5 $\rightarrow$ 0.44 V (24 h)	[74]
		Grafted redox molecular	$\text{H}_2\text{SO}_4 + \text{HQ}$	0 (~3.61 h) $\leftarrow$ 1.0 $\rightarrow$ $\sim$ 0.1 V (~11.11 h)
System optimization	Adding barrier layer	TBAP	1.23 (1 h) $\leftarrow$ 2.0 $\rightarrow$ $\sim$ 1.44 V (1 h)	[85]
	Asymmetric design	$\text{SnSO}_4 + \text{VOSO}_4$	0.92 (10 h) $\leftarrow$ 1.4 $\rightarrow$ $\sim$ 1.16 V (10 h)	[88]

Note: “0 (10 h) $\leftarrow$ 0.8 $\rightarrow$ 0.6 V (10 h)” indicates that the OCV without and with the strategy of suppressing self-discharge decreases from 0.8 V to 0 and 0.6 V after 10 h, respectively.

tion. From this review, one can find that an impactful RE-SC must possess the features of high capacity, high power density, long lifespan, and low self-discharge in a broad temperature range. To achieve this goal, it is necessary to bridge a robust interaction around the electrolyte–electrode interface to balance the common electrochemical performance and self-discharge, which still remains a critical challenge. Herein, several future research directions are suggested.

For separator modification, among ion selectivity modification, charged polarity and PSD optimization, IEM is one of the facile choices to alleviate the shuttle effect. However, the wide applications of IEM are constrained by the high cost. Similar to the blocking layer, the dramatically increased resistance inevitably hinders ion transportation in IEM, thus decreasing the overall electrochemical performance of the device. In contrast, the separators based on electrostatic properties are more effective than PSD adjustment because the interaction between electrode and electrolyte might be tuned easily without pore blocking. More emphasis could be laid on tailor-made polarization of separators and the corresponding effect on the overall electrochemical performance.

Redox additives are extremely important in reconstructing high-performance RE-SCs. Although numerous redox-active species have been investigated for application in aqueous supporting electrolytes, the narrow potential range and rapid ion transport result in medium energy density levels as well as severe self-discharge. Organic electrolytes and ionic liquids can introduce higher voltage and high

base energy density. When coupled with suitable redox-active species, the hybrid electrolytes could impart impressive energy density and lower self-discharge rate. Unfortunately, these nonaqueous supporting electrolytes suffer from low ionic conductivity and high viscosity, resulting in higher equivalent series resistance. Therefore, for the intrinsic nonaqueous electrolyte, one option is the chemical modification on the molecular level to reduce side effects caused by conductivity and viscosity. Moreover, the design and synthesis of new redox-active species with multiple redox centers to match well with the nonaqueous supporting electrolyte must be conducted. The ability of simultaneous reaction on both positive and negative electrodes to balance their energy storage capabilities is urgently required.

A suitable PSD in a porous electrode is important to achieve a high electrochemical ion accessible area, essential for high capacitance and long cycling stability for RE-SCs. Proper PSD is helpful in entrapping redox-active ions inside the pores without obvious pore blocking, conducting to stable energy storage and slow ion shuttle. However, there is not a solid conclusion about the accurate relationship between PSD and the RE-SC’s overall performance. It is difficult to separate the impact of different pores on the electrochemical performance of the device. Compared with the physical confinement by adjusting the PSD of carbon electrodes, the interface interaction between the redox-active ion and electrode surface induced by surface functional groups has a more considerable effect on inhibiting the irreversible shuttle of RE. Different functional groups have different adsorption capabilities for redox



molecules. Therefore, it is of great significance to conduct research on matching between the functional groups and redox molecules. In this respect, accurate control and characterization of electrode–redox additive interaction and how to evaluate the trapping mechanism of redox mediators are needed to get a comprehensive insight into the interface reaction process between the electrode properties and redox species.

Although various indices, namely, capacitance, rate capability, energy/power density, and leakage current or OCV, have been calculated in fundamental research, standardized or universal methods to characterize the RE-SC performance are still missing. Standardization of performance characterization still needs substantial research and development. In addition to ensuring their own basic characteristics, RE-SC systems must also have the potential to integrate with other systems to achieve a wider range of applications. For example, multifunctional RE-SCs can be assembled with the integration of thermal heaters, batteries, piezoelectric, and so forth.

In conclusion, we believe that with the possibility to obtain high energy/power density and long lifetime simultaneously, RE-SCs have the potential to be used as alternative power suppliers for future society if a low self-discharge rate could be achieved through continuous mechanism research and industrial engineering.

## Acknowledgment

The financial support for this work was provided by National Natural Science Foundation of China (52072383, U21A2061, 22209197), Youth Innovation Promotion Association of the Chinese Academy of Sciences (20233432), Natural Science Foundation of Shanxi Province (202203021211002, 202203021222399), and Innovation Fund of Shanxi Institute of Coal Chemistry (SCJC-XCL-2022-08).

## Declaration of conflicting interests

The authors declare no conflicting interests regarding the content of this article.

## References

- [1] Li, Q. Q., Jiang, Y. T., Jiang, Z. M., Zhu, J. Y., Gan, X. M., Qin, F. W., Tang, T. T., Luo, W. X., Guo, N. N., Liu, Z., et al. (2022). Ultrafast pore-tailoring of dense microporous carbon for high volumetric performance supercapacitors in organic electrolyte. *Carbon* 191, 19–27.
- [2] Lin, Q. W., Zhang, J., Lv, W., Ma, J. B., He, Y. B., Kang, F. Y., Yang, Q. H. (2020). A functionalized carbon surface for high-performance sodium-ion storage. *Small* 16, 1902603.
- [3] Zhao, L., He, Y. B., Li, C. F., Jiang, K. L., Wang, P., Ma, J. B., Xia, H. Y., Chen, F. Y., He, Y. B., Chen, Z., et al. (2019). Compact Si/C anodes fabricated by simultaneously regulating the size and oxidation degree of Si for Li-ion batteries. *J. Mater. Chem. A* 7, 24356–24365.
- [4] Guo, X. Y., Zhang, X. S., Wang, Y. X., Tian, X. D., Qiao, Y. (2022). Converting furfural residue wastes to carbon materials for high performance supercapacitor. *Green Energy Environ.* 7, 1270–1280.
- [5] Zhou, H. J., Zhu, G. Y., Dong, S. Y., Liu, P., Lu, Y. Y., Zhou, Z., Cao, S., Zhang, Y. Z., Pang, H. (2023). Ethanol-induced Ni<sup>2+</sup>-intercalated cobalt organic frameworks on vanadium pentoxide for synergistically enhancing the performance of 3D-printed micro-supercapacitors. *Adv. Mater.* 35, 2211523.
- [6] Chen, X. D., Wang, C. L., Wang, Y. H., Ma, J., Dong, Y. J., Gao, S., Jing, Q. L., Li, W. T., Pang, H. (2022). In-situ immobilization cobalt-based metal-organic frameworks nanosheets on carbon composites for supercapacitors. *J. Energy Storage* 55, 105319.
- [7] Lu, J. D., Duan, H. Y., Zhang, Y., Zhang, G. X., Chen, Z. X., Song, Y. Z., Zhu, R. M., Pang, H. (2022). Directional growth of conductive metal–organic framework nanoarrays along [001] on metal hydroxides for aqueous asymmetric supercapacitors. *ACS Appl. Mater. Interfaces* 14, 25878–25885.
- [8] Shao, Y. L., El-Kady, M. F., Sun, J. Y., Li, Y. G., Zhang, Q. H., Zhu, M. F., Wang, H. Z., Dunn, B., Kaner, R. B. (2018). Design and mechanisms of asymmetric supercapacitors. *Chem. Rev.* 118, 9233–9280.
- [9] Liu, Y. F., Du, X. M., Li, Y., Bao, E. H., Ren, X. L., Chen, H. Y., Tian, X. D., Xu, C. J. (2022). Nanosheet-assembled porous MnCo<sub>2</sub>O<sub>4.5</sub> microflowers as electrode material for hybrid supercapacitors and lithium-ion batteries. *J. Colloid Interface Sci.* 627, 815–826.
- [10] Hu, L. T., Zhai, T. Y., Li, H. Q., Wang, Y. G. (2019). Redox-mediator-enhanced electrochemical capacitors: recent advances and future perspectives. *ChemSusChem* 12, 1118–1132.
- [11] Mourad, E., Coustan, L., Lannelongue, P., Zigah, D., Mehdi, A., Vioux, A., Freunberger, S. A., Favier, F., Fontaine, O. (2017). Biredox ionic liquids with solid-like redox density in the liquid state for high-energy supercapacitors. *Nat. Mater.* 16, 446–453.
- [12] Tian, X. D., Yang, T., Song, Y., Li, Y., Peng, H. W., Xue, R. R., Ren, X. Y., Liu, Z. J. (2022). Symmetric supercapacitor operating at 1.5 V with combination of nanosheet-based NiMoO<sub>4</sub> microspheres and redox additive electrolyte. *J. Energy Storage* 47, 103960.
- [13] Evanko, B., Boettcher, S. W., Yoo, S. J., Stucky, G. D. (2017). Redox-enhanced electrochemical capacitors: status, opportunity, and best practices for performance evaluation. *ACS Energy Lett.* 2, 2581–2590.
- [14] Akinwolemiwa, B., Peng, C., Chen, G. Z. (2015). Redox electrolytes in supercapacitors. *J. Electrochem. Soc.* 162, A5054–A5059.
- [15] Li, Y. Y., Cao, R. Y., Song, J. Y., Liang, L., Zhai, T.,

- Xia, H. (2021). Recent advances in coupling carbon-based electrode-redox electrolyte system. *Mater. Res. Bull.* 139, 111249.
- [16] Gorska, B., Frackowiak, E., Beguin, F. (2018). Redox active electrolytes in carbon/carbon electrochemical capacitors. *Curr. Opin. Electrochem.* 9, 95–105.
- [17] Sun, L., Zhuo, K. L., Chen, Y. J., Du, Q. Z., Zhang, S. J., Wang, J. J. (2022). Ionic liquid-based redox active electrolytes for supercapacitors. *Adv. Funct. Mater.* 32, 2203611.
- [18] Yang, N. J., Yu, S. Y., Zhang, W. J., Cheng, H. M., Simon, P., Jiang, X. (2022). Electrochemical capacitors with confined redox electrolytes and porous electrodes. *Adv. Mater.* 34, 2202380.
- [19] Shabangoli, Y., Rahmanifar, M. S., El-Kady, M. F., Noori, A., Mousavi, M. F., Kaner, R. B. (2018). Thionine functionalized 3D graphene aerogel: Combining simplicity and efficiency in fabrication of a metal-free redox supercapacitor. *Adv. Energy Mater.* 8, 1802869.
- [20] Chung, J., Park, H., Jung, C. (2021). Electropolymerizable isocyanate-based electrolytic additive to mitigate diffusion-controlled self-discharge for highly stable and capacitive activated carbon supercapacitors. *Electrochim. Acta.* 369, 137698.
- [21] Tanahashi, I. (2005). Capacitance enhancement of activated carbon fiber cloth electrodes in electrochemical capacitors with a mixed aqueous solution of  $H_2SO_4$  and  $AgNO_3$ . *Electrochem. Solid-State Lett.* 8, A627–A629.
- [22] Sun, X. N., Hu, W., Xu, D., Chen, X. Y., Cui, P. (2017). Integration of redox additive in  $H_2SO_4$  solution and the adjustment of potential windows for improving the capacitive performances of supercapacitors. *Ind. Eng. Chem. Res.* 56, 2433–2443.
- [23] Sun, S., Rao, D. W., Zhai, T., Liu, Q., Huang, H., Liu, B., Zhang, H. S., Xue, L., Xia, H. (2020). Synergistic interface-assisted electrode–electrolyte coupling toward advanced charge storage. *Adv. Mater.* 32, 2005344.
- [24] Byeon, J., Ko, J., Lee, S., Kim, D. H., Kim, S. W., Kim, D., Oh, W., Hong, S., Yoo, S. J. (2023). Solubility-enhancing hydrotrope electrolyte with tailor-made organic redox-active species for redox-enhanced electrochemical capacitors. *ACS Energy Lett.* 8, 2345–2355.
- [25] Kasturi, P. R., Harivignesh, R., Lee, Y. S., Selvan, R. K. (2020). Hydrothermally derived porous carbon and its improved electrochemical performance for supercapacitors using redox additive electrolytes. *J. Phys. Chem. Solids.* 143, 109447.
- [26] Zhang, R., He, X. R. (2015). Crystallization and molecular dynamics of ethylene-vinyl acetate copolymer/butyl rubber blends. *RSC Adv.* 5, 130–135.
- [27] Sun, S., Liu, B., Zhang, H. S., Guo, Q. B., Xia, Q. Y., Zhai, T., Xia, H. (2021). Boosting energy storage via confining soluble redox species onto solid–liquid interface. *Adv. Energy Mater.* 11, 2003599.
- [28] Park, Y., Choi, H., Lee, D. G., Kim, M. C., Tran, N. A. T., Cho, Y., Lee, Y. W., Sohn, J. I. (2020). Rational design of electrochemical iodine-based redox mediators for water-proofed flexible fiber supercapacitors. *ACS Sustainable Chem. Eng.* 8, 2409–2415.
- [29] Tang, X. H., Lui, Y. H., Chen, B. L., Hu, S. (2017). Functionalized carbon nanotube based hybrid electrochemical capacitors using neutral bromide redox-active electrolyte for enhancing energy density. *J. Power Sources* 352, 118–126.
- [30] Wang, G. X., Zhang, M. Y., Xu, H. F., Lu, L., Xiao, Z. Y., Liu, S. (2018). Synergistic interaction between redox-active electrolytes and functionalized carbon in increasing the performance of electric double-layer capacitors. *J. Energy Chem.* 27, 1219–1224.
- [31] Xu, D., Hu, W., Sun, X. N., Cui, P., Chen, X. Y. (2017). Redox additives of  $Na_2MoO_4$  and KI: synergistic effect and the improved capacitive performances for carbon-based supercapacitors. *J. Power Sources* 341, 448–456.
- [32] Sandhiya, M., Vivekanand, Balaji, S. S., Sathish, M. (2021). Unrevealed performance of  $NH_4VO_3$  as a redox-additive for augmenting the energy density of a supercapacitor. *J. Phys. Chem. C.* 125, 8068–8079.
- [33] Chen, K. F., Liu, F., Xue, D. F., Komarneni, S. (2015). Carbon with ultrahigh capacitance when graphene paper meets  $K_3Fe(CN)_6$ . *Nanoscale* 7, 432–439.
- [34] He, Z. Q., Chen, D. D., Wang, M., Li, C. X., Chen, X. Y., Zhang, Z. J. (2020). Sulfur modification of carbon materials as well as the redox additive of  $Na_2S$  for largely improving capacitive performance of supercapacitors. *J. Electroanal. Chem.* 856, 113678.
- [35] Wang, X. F., Chandrabose, R. S., Chun, S. E., Zhang, T. Q., Evanko, B., Jian, Z. L., Boettcher, S. W., Stucky, G. D., Ji, X. L. (2015). High energy density aqueous electrochemical capacitors with a KI-KOH electrolyte. *ACS Appl. Mater. Interfaces* 7, 19978–19985.
- [36] Singh, C., Paul, A. (2018). Immense microporous carbon@hydroquinone metamorphosed from nonporous carbon as a supercapacitor with remarkable energy density and cyclic stability. *ACS Sustainable Chem. Eng.* 6, 11367–11379.
- [37] Xu, D., Sun, X. N., Hu, W., Chen, X. Y. (2017). Carbon nanosheets-based supercapacitors: design of dual redox additives of 1, 4-dihydroxyanthraquinone and hydroquinone for improved performance. *J. Power Sources* 357, 107–116.
- [38] Calcagno, G., Evanko, B., Stucky, G. D., Ahlberg, E., Yoo, S. J., Palmqvist, A. E. C. (2022). Understanding the operating mechanism of aqueous pentyl viologen/bromide redox-enhanced electrochemical capacitors with ordered mesoporous carbon electrodes. *ACS Appl. Mater. Interfaces* 14, 20349–20357.
- [39] Hu, L. T., Shi, C., Guo, K., Zhai, T. Y., Li, H. Q., Wang, Y. G. (2018). Electrochemical double-layer capacitor energized by adding an ambipolar organic redox radical into the electrolyte. *Angew. Chem. Int. Ed.* 57, 8214–8218.
- [40] Zhang, Y., Zeng, T., Yan, W., Huang, D. X., Zhang,

- Y. Y., Wan, Q. J., Yang, N. J. (2022). A high-performance flexible supercapacitor using dual alkaline redox electrolytes. *Carbon* 188, 315–324.
- [41] Zhai, D. D., Liu, H., Wang, M., Wu, D., Chen, X. Y., Zhang, Z. J. (2019). Integrating surface functionalization and redox additives to improve surface reactivity for high performance supercapacitors. *Electrochim. Acta.* 323, 134810.
- [42] Zhang, X., Gao, L. L., Guo, R. H., Hu, T. P., Ma, M. M. (2021). Using thiourea as a catalytic redox-active additive to enhance the performance of pseudocapacitive supercapacitors. *Sustainable Energy Fuels* 5, 5733–5740.
- [43] Yoon, H., Kim, H. J., Yoo, J. J., Yoo, C. Y., Park, J. H., Lee, Y. A., Cho, W. K., Han, Y. K., Kim, D. H. (2015). Pseudocapacitive slurry electrodes using redox-active quinone for high-performance flow capacitors: an atomic-level understanding of pore texture and capacitance enhancement. *J. Mater. Chem. A* 3, 23323–23332.
- [44] Xiong, T., Lee, W. S. V., Chen, L., Tan, T. L., Huang, X. L., Xue, J. M. (2017). Indole-based conjugated macromolecules as a redox-mediated electrolyte for an ultrahigh power supercapacitor. *Energy Environ. Sci.* 10, 2441–2449.
- [45] Park, J., Kim, B., Yoo, Y. E., Chung, H., Kim, W. (2014). Energy-density enhancement of carbon-nanotube-based supercapacitors with redox couple in organic electrolyte. *ACS Appl. Mater. Interfaces* 6, 19499–19503.
- [46] Wang, Z. F., Yi, Z. L., Yu, S. C., Fan, Y. F., Li, J. X., Xie, L. J., Zhang, S. C., Su, F. Y., Chen, C. M. (2022). High-voltage redox mediator of an organic electrolyte for supercapacitors by lewis base electrocatalysis. *ACS Appl. Mater. Interfaces* 14, 24497–24508.
- [47] Shakil, R., Shaikh, M. N., Shah, S. S., Reaz, A. H., Roy, C. K., Chowdhury, A. N., Aziz, M. A. (2021). Development of a novel bio-based redox electrolyte using pivalic acid and ascorbic acid for the activated carbon-based supercapacitor fabrication. *Asian J. Org. Chem.* 10, 2220–2230.
- [48] Navalpotro, P., Palma, J., Anderson, M., Marcilla, R. (2016). High performance hybrid supercapacitors by using para-benzoquinone ionic liquid redox electrolyte. *J. Power Sources* 306, 711–717.
- [49] Xie, H. J., Gélinas, B., Rochefort, D. (2016). Redox-active electrolyte supercapacitors using electroactive ionic liquids. *Electrochem. Commun.* 66, 42–45.
- [50] Shang, W. X., Yu, W. T., Xiao, X., Ma, Y. Y., He, Y., Zhao, Z. X., Tan, P. (2023). Insight into the self-discharge suppression of electrochemical capacitors: Progress and challenges. *Adv. Powder Mater.* 2, 100075.
- [51] Jamieson, L., Roy, T., Wang, H. Z. (2021). Postulation of optimal charging protocols for minimal charge redistribution in supercapacitors based on the modelling of solid phase charge density. *J. Energy Storage* 40, 102716.
- [52] Shen, J. F., He, Y. J., Ma, Z. F. (2016). A systematic evaluation of polynomial based equivalent circuit model for charge redistribution dominated self-discharge process in supercapacitors. *J. Power Sources* 303, 294–304.
- [53] Lewandowski, A., Jakobczyk, P., Galinski, M., Biegun, M. (2013). Self-discharge of electrochemical double layer capacitors. *Phys. Chem. Chem. Phys.* 15, 8692–8699.
- [54] Andreas, H. A. (2015). Self-discharge in electrochemical capacitors: a perspective article. *J. Electrochem. Soc.* 162, A5047–A5053.
- [55] Xia, M. Y., Nie, J. H., Zhang, Z. L., Lu, X. M., Wang, Z. L. (2018). Suppressing self-discharge of supercapacitors via electrorheological effect of liquid crystals. *Nano Energy* 47, 43–50.
- [56] Wang, K. P., Yao, L. L., Jahon, M., Liu, J. X., Gonzalez, M., Liu, P., Leung, V., Zhang, X. Y., Ng, T. N. (2020). Ion-exchange separators suppressing self-discharge in polymeric supercapacitors. *ACS Energy Lett.* 5, 3276–3284.
- [57] Lee, J., Choudhury, S., Weingarth, D., Kim, D., Presser, V. (2016). High performance hybrid energy storage with potassium ferricyanide redox electrolyte. *ACS Appl. Mater. Interfaces* 8, 23676–23687.
- [58] Peng, H., Xiao, L. L., Sun, K. J., Ma, G. F., Wei, G. G., Lei, Z. Q. (2019). Preparation of a cheap and environmentally friendly separator by coaxial electrospinning toward suppressing self-discharge of supercapacitors. *J. Power Sources* 435, 226800.
- [59] Buxton, W. G., King, S. G., Stolojan, V. (2023). Suppression of self-discharge in aqueous supercapacitor devices incorporating highly polar nanofiber separators. *Energy Environ. Mater.* 6, e12363.
- [60] Yu, X. W., Wu, H., Koo, J. H., Manthiram, A. (2020). Tailoring the pore size of a polypropylene separator with a polymer having intrinsic nanoporosity for suppressing the polysulfide shuttle in lithium–sulfur batteries. *Adv. Energy Mater.* 10, 1902872.
- [61] Liang, N., Wu, X. Y., Lv, Y., Guo, J. X., Zhang, X. L., Zhu, Y. F., Liu, H. B., Jia, D. Z. (2022). A graphdiyne oxide composite membrane for active electrolyte enhanced supercapacitors with super long self-discharge time. *J. Mater. Chem. C* 10, 2821–2827.
- [62] Chen, L. B., Bai, H., Huang, Z. F., Li, L. (2014). Mechanism investigation and suppression of self-discharge in active electrolyte enhanced supercapacitors. *Energy Environ. Sci.* 7, 1750–1759.
- [63] Chun, S. E., Evanko, B., Wang, X. F., Vonlanthen, D., Ji, X. L., Stucky, G. D., Boettcher, S. W. (2015). Design of aqueous redox-enhanced electrochemical capacitors with high specific energies and slow self-discharge. *Nat. Commun.* 6, 7818.
- [64] Evanko, B., Yoo, S. J., Chun, S. E., Wang, X. F., Ji, X. L., Boettcher, S. W., Stucky, G. D. (2016). Efficient charge storage in dual-redox electrochemical capacitors through reversible counterion-induced solid complexation. *J. Am. Chem. Soc.* 138, 9373–9376.
- [65] Yoo, S. J., Evanko, B., Wang, X. F., Romelczyk, M.,

- Taylor, A., Ji, X. L., Boettcher, S. W., Stucky, G. D. (2017). Fundamentally addressing bromine storage through reversible solid-state confinement in porous carbon electrodes: design of a high-performance dual-redox electrochemical capacitor. *J. Am. Chem. Soc.* 139, 9985–9993.
- [66] Haque, M., Li, Q., Smith, A. D., Kuzmenko, V., Rudquist, P., Lundgren, P., Enoksson, P. (2020). Self-discharge and leakage current mitigation of neutral aqueous-based supercapacitor by means of liquid crystal additive. *J. Power Sources* 453, 227897.
- [67] Su, X. L., Jia, W. S., Ji, H. X., Zhu, Y. W. (2021). Mitigating self-discharge of activated carbon-based supercapacitors with hybrid liquid crystal as an electrolyte additive. *J. Energy Storage* 41, 102830.
- [68] Shi, M. W., Zhang, Z. L., Zhao, M., Lu, X. M., Wang, Z. L. (2021). Reducing the self-discharge rate of supercapacitors by suppressing electron transfer in the electric double layer. *J. Electrochem. Soc.* 168, 120548.
- [69] Wang, H. Y., Chen, J. Y., Fan, R. X., Wang, Y. (2018). A flexible dual solid-state electrolyte supercapacitor with suppressed self-discharge and enhanced stability. *Sustainable Energy Fuels* 2, 2727–2732.
- [70] Hor, A. A., Yadav, N., Hashmi, S. A. (2022). High energy density carbon supercapacitor with ionic liquid-based gel polymer electrolyte: role of redox-additive potassium iodide. *J. Energy Storage* 47, 103608.
- [71] Wang, Z. X., Chu, X., Xu, Z., Su, H., Yan, C., Liu, F. Y., Gu, B. N., Huang, H. C., Xiong, D., Zhang, H. P., et al. (2019). Extremely low self-discharge solid-state supercapacitors via the confinement effect of ion transfer. *J. Mater. Chem. A* 7, 8633–8640.
- [72] Wang, B., Wang, C. H., Hu, Q., Zhang, L., Wang, Z. Y. (2020). Modeling the dynamic self-discharge effects of supercapacitors using a controlled current source based ladder equivalent circuit. *J. Energy Storage* 30, 101473.
- [73] Zhao, M., Shi, M. W., Zhou, H. H., Zhang, Z. L., Yang, W., Ma, Q., Lu, X. M. (2021). Self-discharge of supercapacitors based on carbon nanosheets with different pore structures. *Electrochim. Acta.* 390, 138783.
- [74] Zhang, W., Yang, W., Zhou, H. H., Zhang, Z. L., Zhao, M., Liu, Q., Yang, J., Lu, X. M. (2020). Self-discharge of supercapacitors based on carbon nanotubes with different diameters. *Electrochim. Acta.* 357, 136855.
- [75] Lee, J., Srimuk, P., Fleischmann, S., Ridder, A., Zeiger, M., Presser, V. (2017). Nanoconfinement of redox reactions enables rapid zinc iodide energy storage with high efficiency. *J. Mater. Chem. A* 5, 12520–12527.
- [76] Zhao, Y., Taylor, E. E., Hu, X. D., Evanko, B., Zeng, X. J., Wang, H. B., Ohnishi, R., Tsukazaki, T., Li, J. F., Stadie, N. P., et al. (2021). What structural features make porous carbons work for redox-enhanced electrochemical capacitors? A fundamental investigation. *ACS Energy Lett.* 6, 854–861.
- [77] Schweizer, S., Landwehr, J., Etzold, B. J. M., Meißner, R. H., Amkreutz, M., Schiffels, P., Hill, J. R. (2019). Combined computational and experimental study on the influence of surface chemistry of carbon-based electrodes on electrode–electrolyte interactions in supercapacitors. *J. Phys. Chem. C.* 123, 2716–2727.
- [78] Ike, I. S., Sigalas, I., Iyuke, S. (2016). Understanding performance limitation and suppression of leakage current or self-discharge in electrochemical capacitors: a review. *Phys. Chem. Chem. Phys.* 18, 661–680.
- [79] Yan, L. J., Li, D., Yan, T. T., Chen, G. R., Shi, L. Y., An, Z. X., Zhang, D. S. (2018). Confining redox electrolytes in functionalized porous carbon with improved energy density for supercapacitors. *ACS Appl. Mater. Interfaces* 10, 42494–42502.
- [80] Shul, G., Bélanger, D. (2016). Self-discharge of electrochemical capacitors based on soluble or grafted quinone. *Phys. Chem. Chem. Phys.* 18, 19137–19145.
- [81] Cao, R. Y., Zhang, Y., Du, Y. N., Zeng, Y. Y., Yu, M. H., Zhai, T., Xia, H. (2021). Coupling electrode-redox electrolyte within carbon nanotube arrays for supercapacitors with suppressed self-discharge. *Sustainable Mater. Technol.* 28, e00284.
- [82] Mai, L. Q., Minhas-Khan, A., Tian, X. C., Hercule, K. M., Zhao, Y. L., Lin, X., Xu, X. (2013). Synergistic interaction between redox-active electrolyte and binder-free functionalized carbon for ultrahigh supercapacitor performance. *Nat. Commun.* 4, 2923.
- [83] Isikli, S., Lecea, M., Ribagorda, M., Carreño, M. C., Díaz, R. (2014). Influence of quinone grafting via friedel–crafts reaction on carbon porous structure and supercapacitor performance. *Carbon* 66, 654–661.
- [84] Sheng, L. Z., Jiang, L. L., Wei, T., Liu, Z., Fan, Z. J. (2017). Spatial charge storage within honeycomb-carbon frameworks for ultrafast supercapacitors with high energy and power densities. *Adv. Energy Mater.* 7, 1700668.
- [85] Tevi, T., Yaghoubi, H., Wang, J., Takshi, A. (2013). Application of poly (p-phenylene oxide) as blocking layer to reduce self-discharge in supercapacitors. *J. Power Sources* 241, 589–596.
- [86] Hamed, S., Ghanbari, T., Moshksar, E., Hosseini, Z. (2021). Time-varying model of self-discharge in a double layer supercapacitor with blocking layer. *J. Energy Storage* 40, 102730.
- [87] Frackowiak, E., Fic, K., Meller, M., Lota, G. (2012). Electrochemistry serving people and nature: High-energy ecocapacitors based on redox-active electrolytes. *ChemSusChem* 5, 1181–1185.
- [88] Lee, J., Krüner, B., Tolosa, A., Sathyamoorthi, S., Kim, D., Choudhury, S., Seo, K. H., Presser, V. (2016). Tin/vanadium redox electrolyte for battery-like energy storage capacity combined with supercapacitor-like power handling. *Energy Environ. Sci.* 9, 3392–3398.